Received: 18 November 2021 | Accepted: 22 November 2021

DOI: 10.1002/ecs2.4022

ECOSPHERE
AN ESA OPEN ACCESS JOURNAL

ARTICLE

Coastal and Marine Ecology

Coastal infrastructure alters behavior and increases predation mortality of threatened Puget Sound steelhead smolts

Megan E. Moore | **Barry A. Berejikian**

Environmental and Fisheries Sciences, Northwest Fisheries Science Center, National Oceanic and Atmospheric Administration, Port Orchard, Washington, USA

Correspondence
Megan E. Moore
Email: megan.moore@noaa.gov

Funding information
NOAA; State of Washington; Salmon Recovery Funding Board

Handling Editor: F. Joel Fodrie

Abstract

Fundamental movements of migratory species can be substantially influenced by marine habitat disruptions caused by coastal infrastructure. The Hood Canal Bridge (HCB) spans the northern outlet of Hood Canal in the Salish Sea, extends 4.6 m (15 ft) underwater, and forms a partial barrier for steelhead migrating from Hood Canal to the Pacific Ocean. Spatial mark–recapture survival models using acoustic telemetry data indicate that only 49% (2017; 95% confidence interval (CI) = 40%–58%) and 56% (2018; 95% CI = 48%–65%) of the steelhead smolts encountering the HCB survived past the bridge and 7 km to the next array. We studied fine-scale movements of more than 300 steelhead smolts to understand how migration behavior was affected across the entire length of the HCB and to quantify spatial and temporal patterns of mortality. Individually coded acoustic telemetry transmitters implanted in juvenile steelhead were used in conjunction with an extensive array of acoustic receivers surrounding the HCB to obtain approximations of the path each steelhead took as they encountered the bridge structure. Steelhead survival past the HCB appeared unaffected by tidal stage, population-of-origin, approach location, current velocity, or time of day, but was influenced by week of bridge encounter. Behavioral data from transmitters with temperature and depth sensors ingested by predators are consistent with high levels of marine mammal predation. This study confirms the considerable impact of the HCB on Endangered Species Act-listed steelhead smolt survival, and provides detailed information on the behavior of steelhead smolts and their predators at the HCB for use in planning recovery actions.

KEYWORDS
habitat connectivity, migration, predation, steelhead, transportation infrastructure

INTRODUCTION

Until very recently in human history, structures built for human convenience were installed with little regard to the harm they might impose on surrounding ecosystems, and have collectively led to widespread fragmentation across habitats (Bulleri & Chapman, 2010; Crooks et al., 2017; Haddad et al., 2015). Today, modern ecological investigations demonstrate the importance of habitat connectivity for maintaining key biological conservation metrics, including biodiversity and productivity (Olds et al., 2016; Polis et al., 1997; Vargas-Fonseca et al., 2016). Fundamentally, habitat connectivity allows individuals to move between habitats and successfully carry out essential life functions (Gillanders et al., 2003; Sheaves, 2009).

For migratory species, the importance of connectivity extends to a broad scale where large swathes of continuous habitat are required to complete an entire life cycle. The extensive use of dams to provide hydropower, irrigation, and transportation in river systems provides a clear example of physical habitat disruption (Hall et al., 2011; Nilsson et al., 2005), impacting aquatic migratory species in particular (Drinkwater & Frank, 1994; Nehlsen et al., 1991). Dams interrupt species migrations and isolate habitat patches in much the same way roads bisect and fragment terrestrial ecosystems (Shepard et al., 2008; Trombulak & Frissell, 2000). Development in coastal marine ecosystems can create partial habitat fragmentation that may have less obvious, underwater impacts. Human-built infrastructure in the form of seawalls, piers, docks, or bridges can decouple terrestrial and marine ecosystem interactions (Sobocinski et al., 2010; Toft et al., 2007), alter migration behavior (Celedonia et al., 2008; Munsch et al., 2014), increase predator impacts on prey species (Yurk & Trites, 2000), and reduce biodiversity (Chapman, 2003). Oceanic currents, water temperatures, land boundaries, bathymetry, and seabed type can be important factors in determining animal movement patterns (Bestley et al., 2012; Gaspar & Lalire, 2017; Meckley et al., 2017). Disruption of these movement cues may decrease the ability of marine species to migrate successfully.

Pacific salmon and steelhead (*Oncorhynchus* spp.) native to the West Coast of North America exhibit an anadromous life history, and are thus dependent on habitat connectivity from natal streams to the open ocean. The Salish Sea straddles the US–Canada border and includes the Strait of Juan de Fuca (JDF), the Strait of Georgia, and Puget Sound, a network of inland waters in Northwestern Washington State. Several salmonid species in Puget Sound have experienced declines in abundance over the last three decades, resulting in multiple listings under the Endangered Species Act (ESA). Interannual variation in marine survival rates for a number of Salish Sea salmon and steelhead populations appears linked to factors occurring soon after initial marine entry (Kendall et al., 2017; Ruff et al., 2017; Zimmerman et al., 2015). Steelhead (*Oncorhynchus mykiss*) populations listed as Threatened under the US ESA (72 FR 26722, 11 May 2007) experience low survival rates as they migrate through Puget Sound, limiting productivity and impeding recovery (Moore et al., 2015; Moore & Berejikian, 2017; National Marine Fisheries Service, 2019). Puget Sound steelhead smolt-to-adult marine survival rates are strongly, negatively related to harbor seal (*Phoca vitulina*) abundance (Sobocinski et al., 2020), and pinniped (i.e., seals and sea lions) predation is thought to be an important factor limiting the marine survival of other imperiled salmonid populations as well (Chasco et al., 2017; Nelson et al., 2019; Wargo Rub et al., 2019).

Several salmonid species, including ESA-threatened steelhead, ESA-endangered summer chum salmon (*O. keta*), ESA-threatened Chinook salmon (*O. tswaytscha*), and coho salmon (*O. kisutch*) originating in rivers feeding into Hood Canal (a subbasin of Puget Sound), must migrate past the Hood Canal Bridge (HCB) to continue their life cycle in the Pacific Ocean. However, the HCB floats on continuous concrete pontoons that extend 4.6 m beneath the surface and occupy approximately 90% of the width of Hood Canal. Elevated approaches from the shorelines to the floating section span the remaining 10% of the canal width. Despite unobstructed nearshore corridors, migration delays at the bridge contribute to increased mortality of steelhead smolts attempting passage (Moore & Berejikian, 2013). The submerged pontoons also inhibit natural tidal flow and disrupt natural currents, altering local salinity and temperature profiles (Khangaonkar et al., 2018) that may influence movements of other anadromous salmonid species.

To understand how habitat disruption caused by the HCB impacts Puget Sound steelhead, we used acoustic telemetry to conduct an intensive quantitative assessment of the survival and behavior of steelhead outmigrants. For the past two decades, researchers have implanted miniaturized acoustic transmitters in and tracked salmonids along migration routes using broad-scale receiver arrays to discover patterns of behavior and survival in the wild (Lacroix et al., 2004; Perry et al., 2010; Welch et al., 2009). Fine-scale receiver arrays are used less frequently but yield rich, detailed behavioral data (Celedonia et al., 2008; Leander et al., 2021; Steel et al., 2013). Previous acoustic telemetry work documenting mortality at the HCB from 2006 to 2010 lacked the precision to determine individual fish locations or discern the cause of smolt mortality (Moore & Berejikian, 2013). The current study deployed a more extensive and dense acoustic telemetry array on both sides of the HCB and at sites throughout the steelhead migration route, providing the precise fish location data to (1) estimate the impact of the HCB on survival, (2) identify physical and biological factors contributing to migration delay and low survival, (3) map spatial patterns of movement and mortality, and (4) identify potential predator species based on the behavior of acoustic transmitters near the HCB.

METHODS

Study area

The Hood Canal is a 110-km-long fjord, forming a subbasin of Puget Sound in Northwest Washington State, USA (Figure 1), with an average width of 2.4 km and mean depth of 51.1 m. Natural- and hatchery-origin salmonids migrate to and from streams feeding into Hood Canal, including populations of Chinook, chum, coho, sockeye (*O. nerka*), and pink (*O. gorbuscha*) salmon, and steelhead and cutthroat trout (*O. clarkii*). The HCB spans a narrowing of Hood Canal near the northern outlet, providing a transportation connection between the Olympic and Kitsap Peninsulas. Perpendicular floating pontoons cross the primary linear pontoons at the approach spans and support the drawspan that retracts to allow passage of vessel traffic (Figure 2).

Fish tagging

Wild steelhead smolts were collected from a rotary screw trap in the South Fork Skokomish River (river kilometer, rkm, 13.5) and a weir trap in Big Beef Creek (rkm 0.1) during April and May of 2017 and 2018 (Figure 1). Captured smolts were held in flow-through circular tanks for 1–48 (typically <24) h prior to tagging. Steelhead smolts were anesthetized using MS-222 infused river water (40 mg/L) and surgically implanted with one of four types of Vemco (now InnovaSea Systems Inc., hereafter InnovaSea; https://www.innovasea.com/fish-tracking/) 69 kHz transmitters: (1) V8-4x (8 mm diameter × 20.5 mm length, 2.0 g, 90-day expected battery life), (2) V9P-6 L (9 × 31 mm, 4.9 g, equipped with pressure sensor, 95 days), (3) V7P-4H (7 × 24 mm, 2.0 g, equipped with pressure sensor, 51 days), (4) V7T-4H (7 × 34 mm, 2.0 g, equipped with temperature sensor, 51 days), or (5) "delay" V8-4x (8 mm diameter × 20.5 mm length, 2.0 g, 95 days; Table 1). The incision was closed with two interrupted triple knot stitches using sterile monofilament (Ethicon Monocryl 5-0 monofilament, with a 3/8 circle, reverse-cutting 13-mm needle). All transmitters were programmed to ping continuously at random intervals between 30 and 90 s. An additional 49 "delay" V8 transmitters were programmed to be off for the first 8 days after release then on for the remainder of transmitter life, and were deployed to test the null hypothesis that the survival rate of tagged steelhead emitting a signal at 69 kHz did not differ from the survival rate of steelhead with silent transmitters. No difference in survival was observed between delay- and continuous-tagged smolts (M. Moore, unpublished data). InnovaSea V7 and V9 pressure sensors recorded the depth (maximum depth = 38 m, but the sensor continued to record max depth if deeper), and temperature sensors recorded the ambient temperature (range = −5 to 35°C) of the tagged animal when within range of a receiver. Tagged steelhead were held for 20–30 h after surgery in flow-through 200-L tanks then released at the location of capture.

Receiver deployment

A network of InnovaSea receivers was deployed at various locations along the steelhead outmigration route to record the unique signal of each tagged smolt as it migrated from river mouths (RMs) to the Pacific Ocean (Figure 1). Receiver arrays were deployed to estimate survival and provide fine-scale behavior patterns within approximately 250 m on either side of the HCB. Two VR2W receivers were installed at the RMs of the Skokomish River and Big Beef Creek to detect tagged smolts entering the marine waters of Hood Canal. An InnovaSea Vemco positioning system (VPS) comprised of 24 VR2AR and three VR2W receivers (69 kHz; capable of decoding the signal from InnovaSea acoustic transmitters) in 2017 (5 March–1 August), and 28 VR2AR and 14 VR2W receivers in (6 March–13 September) 2018, was configured and deployed to provide fine-scale spatial information on tagged steelhead at the HCB (Figure 1). The VPS system uses an array of receivers equipped with co-located transmitters to communicate the instrument location to other system receivers. Receivers were deployed in close proximity to each other to facilitate detection of a single transmission by multiple receivers, which enabled triangulation of each transmitter as it moved through the array. Stationary reference transmitters (five transmitters in 2017 and four transmitters in 2018) were deployed within the system to test the accuracy and precision of the VPS system each year. Four additional VR2AR receivers were deployed approximately 600 m apart at Twin Spits (TS), 7 km north of the HCB, to determine whether smolts migrated successfully past the HCB. In all, 12 InnovaSea VR3 receivers spanned Admiralty Inlet (ADM) and a final line of 29 InnovaSea VR3 and VR4 receivers (maintained by the Ocean Tracking Network; https://oceantrackingnetwork.org/) spanned the Strait of JDF at Pillar Point (Figure 1).

Data processing

All receiver files were downloaded from recovered receivers or via surface modem (VR3s and VR4s) and compiled into a database. Raw data from single line receiver arrays were used for analyses requiring only

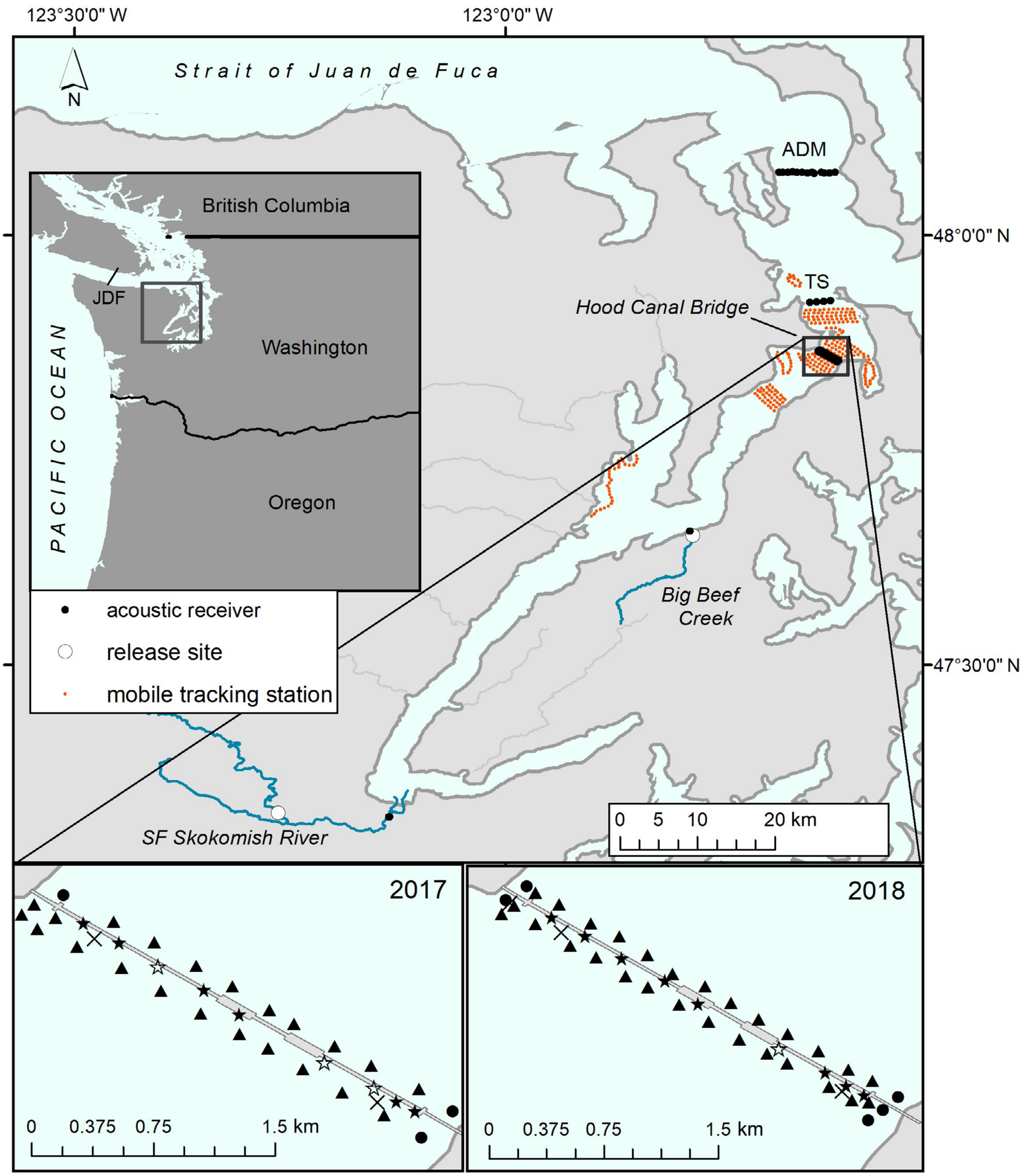

FIGURE 1 Map of the Hood Canal study area showing receiver locations (black dots) at the mouths of Big Beef Creek and the Skokomish River, the Hood Canal Bridge, at Twin Spits (TS), at Admiralty Inlet (ADM), and the Strait of Juan de Fuca (JDF, black line). Lower insets show locations of VR2AR receivers (black triangles), seabed-moored VR2W receivers (black circles), seabed-moored VR2W receivers with co-located reference transmitter (open stars), VR2W receivers hanging from the bridge railing (black stars), and seabed-moored reference transmitters (black X) used to calibrate the Vemco positioning system (VPS) in 2017 and 2018

presence or absence information. Files from the VPS array receivers were used to generate precise transmitter positions.

InnovaSea processed VPS receiver detection data using hyperbolic positioning techniques (Smith, 2013). Briefly, hyperbolic positioning measures differences in transmission detection times between pairs of time-synchronized receivers, then converts the time differences to distance values using the signal propagation speed, allowing for triangulation of a transmitter position. VPS analysis returned the coordinates and date–time of each tagged animal as it moved through the array, coordinates and date-time of the reference transmissions throughout the length of each deployment, and an estimate of accuracy for each position

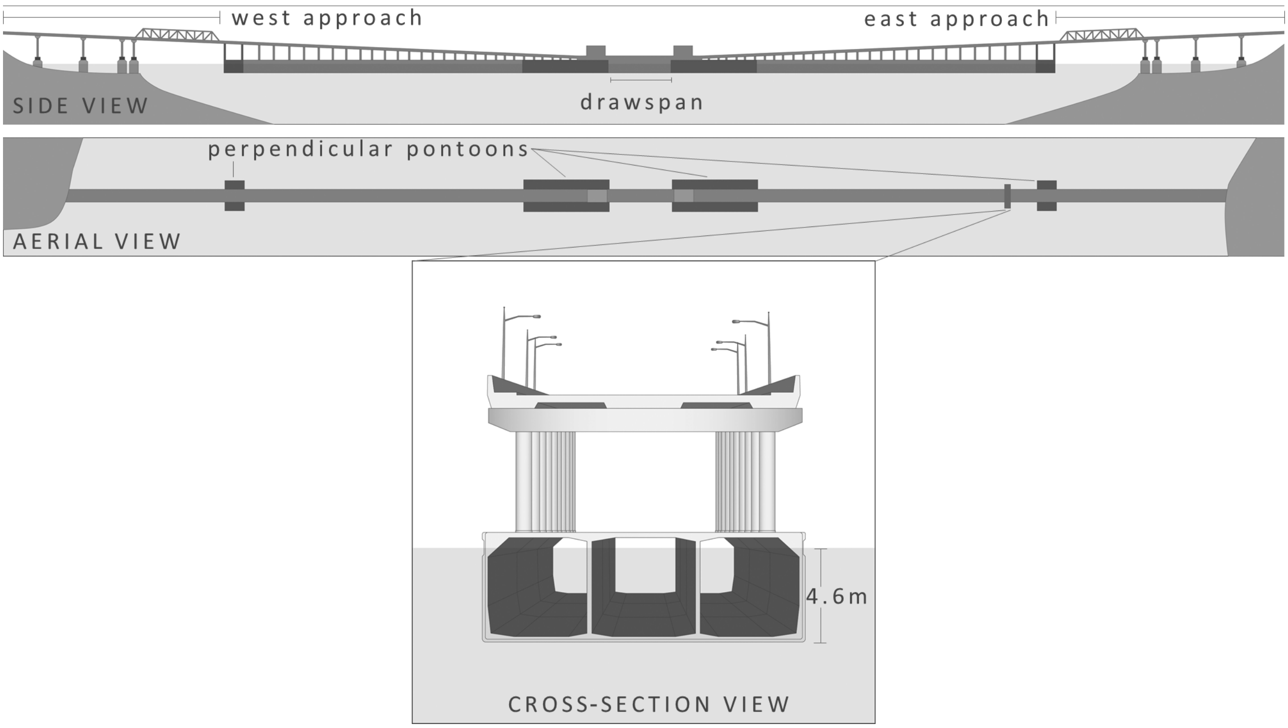

FIGURE 2 Conceptual drawing of the side, aerial, and cross-section views of the Hood Canal Bridge (not drawn to scale)

TABLE 1 The number and size of steelhead smolts from Big Beef Creek (BBC) and the Skokomish River tagged with acoustic transmitters

Transmitter type	Number tagged	Length (mm)	Weight (g)
2017			
BBC V8	61	183 ± 2	57 ± 2
BBC V9P	40	223 ± 4	107 ± 7
Skokomish V8	89	175 ± 1	50 ± 1
Skokomish V9P	9	209 ± 3	86 ± 3
Total	248	188 ± 2	64 ± 2
2018			
BBC V8	92	175 ± 2	51 ± 3
BBC V7P	29	185 ± 5	61 ± 6
BBC V7T	28	185 ± 5	61 ± 5
Skokomish V8	58	166 ± 2	42 ± 1
Skokomish V7P	21	187 ± 6	56 ± 4
Skokomish V7T	22	181 ± 3	55 ± 2
Total	250	177 ± 1	52 ± 1

Note: Values for length and weight are expressed as mean ± SE.

that is unique to each VPS array. To calculate error, the VPS analysis software uses the known positions of the reference transmitters to measure the distance between the triangulated position and the true position (HPEm), then calculates a second error estimate (HPE) that incorporates variation based on receiver array geometry and effects of depth, temperature, and salinity on the speed of signal transmission. However, the true location is only known for reference transmitters and not for animal transmitters, so the relationship between HPEm and HPE can only be examined for reference transmitters then subsequently applied to animal positions (Espinoza et al., 2011; Roy et al., 2014). For both VPS arrays separately, we created bins for all HPE values and plotted them against median HPEm values. Where there was a steep increase in median HPEm, we defined a threshold (same for both years) and deleted animal detections with HPE values larger than that threshold. After applying this filter, 96.2% (2017) and 87.6% (2018) of the animal positions were retained. Median HPEm values for identically filtered reference transmitter data were 4.4 m in 2017 and 5.0 m in 2018. These accuracy estimates can be applied to animal position data because HPE was calculated in the same way for both reference and animal transmitters. Processed data from all tagged animals were plotted for further analysis using ArcGIS 10.5.1 (Redlands, CA).

Data analysis

Survival estimation

Segment-specific survival of tagged steelhead smolts was estimated using separate Cormack–Jolly–Seber (CJS) mark–

recapture models for 2017 and 2018 detection data (Cormack, 1964; Jolly, 1965; Seber, 1965), adapted for spatial rather than temporal encounter information (e.g., Burnham et al., 1987; Skalski et al., 2001). The R (version 3.6.2; R Core Team, 2019) package "RMark" (Laake, 2013) was used to construct and test models to jointly estimate both apparent survival (hereafter "survival"; ϕ) and detection probability (*p*) in concert with the program Mark (White & Burnham, 1999). Presence or absence of all transmitters (except V8 delay transmitters) at each receiver array were compiled to create encounter histories. We assumed that all initial transmitter detections at an array were in a live smolt, because records of all predation events based on behavioral change at the HCB indicated that the transmitter was in a steelhead upon approach (see "*Locating predation events*"). In CJS models, mortality and residualism (i.e., failure to migrate within the primary temporal window) are confounded, but previous telemetry work has shown no evidence to suggest that steelhead remain in Hood Canal or Puget Sound beyond August when arrays were downloaded (Moore et al., 2010, 2015). Models were structured to estimate ϕ from release (REL) to RM (ϕ_{REL-RM}), RM to the HCB (ϕ_{RM-HCB}), HCB to TS (ϕ_{HCB-TS}), TS to ADM (ϕ_{TS-ADM}), and ADM to the Strait of JDF ($\phi_{ADM-JDF}$) in 2017. In 2018, our transmitters were not compatible with the ADM receiver code maps, so we combined ϕ_{TS-ADM} and $\phi_{ADM-JDF}$ to estimate ϕ_{TS-JDF} (Figure 1). Transmitter-specific values for *p* at JDF (V7 = 0.69; V8 and V9 = 0.91) were fixed according to regression model-predicted $\hat{p}$ of similarly spaced ocean acoustic receiver arrays to isolate the confounded ϕ and *p* at the final encounter location (see appendix A in Melnychuk, 2009).

We took a two-phase approach to modeling ϕ and *p*, using Akaike information criteria for finite sample sizes (AIC_c) to identify the best models in each phase. Assuming separate parameters for all ϕ segments and all receiver array-specific *p*, Phase 1 compared a simple segment-varying model (ϕ(segment), *p*(array)) to models that incorporated additional effects of transmitter type (V8, V9P, V7P, or V7T) on *p* and differences in ϕ_{REL-RM} and ϕ_{RM-HCB} by population since longer distances were covered by Skokomish smolts during these first two migration segments. The effect of the HCB on survival was of primary interest, so Phase 2 model comparisons took the model with the lowest AIC_c from the first phase and compared models with additional effects on ϕ_{HCB-TS}. Covariates tested individually in the second phase models included: length (fork length of each tagged smolt), transmitter type, week of first detection at HCB (2017: 9 April [Week 15]–3 June [Week 22]; 2018: 8 April [Week 15]–9 June [Week 23]), HCB approach location (determined by the receiver location of the first detection, modeled as a factor variable with two levels [side or middle] because the side approach spans provide unobstructed surface water; Figure 2), tidal stage (ebb or flow) at time of first HCB bridge detection, predicted current velocity (6-min resolution data from HCB station PUG1603; https://tidesandcurrents.noaa.gov/noaacurrents/Predictions?id=PUG1603_20) at time of first HCB detection, and a two-level factor variable for whether the first detection at the HCB occurred during the day or at night (based on time of sunset and sunrise).

Goodness-of-fit-was assessed by assessing Fletcher's c-hat (Fletcher, 2012). Estimated c-hat was found to be 1.2 for the null 2017 mark–recapture model, so model comparison tables were adjusted accordingly. Models using 2018 data showed no evidence of overdispersion (c-hat ≈ 1.00), so no adjustments were made.

To compare behavioral patterns of smolts that successfully migrated past the HCB to those of unsuccessful migrants, tagged smolts were classified as survivors if they were detected at the TS receiver array ($p_{2017} = 0.98$, $p_{2018} = 0.94$), or at any other array further along the migration route. Tagged smolts were classified as non-survivors, or "mortalities," if they were not detected after the HCB (Figure 1).

Travel and residence times

Travel times were calculated by subtracting the date and time of each transmitter's last detection at the first receiver array along the migration route from the date and time of the last detection at the subsequent receiver array. Travel distances were measured as the minimum straight line distance from the center of one receiver array to the next. Time spent at the HCB (HCB time) was calculated as the time between the first and last detection at any HCB array receiver. To calculate continuous HCB time, we subtracted all time greater than 24 h during which a transmitter was not heard on any receivers. Travel time for the entire marine migration (RM-JDF) was calculated by summing average travel times for each migration segment (RM-JDF = RM-HCB + $HCB_{initial} - HCB_{final}$ + HCB-TS + TS-ADM + ADM-JDF).

Stationary transmitters

Mobile tracking at stations surrounding the HCB was performed using an InnovaSea VR100 and 69 kHz omnidirectional hydrophone suspended approximately 3 m under the surface of the water. A set of 261 stations was designed to monitor (1) the area immediately adjacent to the HCB, (2) areas on the migration route distant from the HCB and less influenced by it, and (3) known areas of predator aggregation (Figure 1). After the conclusion of the typical smolt migration period, we listened for 4 min at each station in both 2017 and 2018, recording any decoded transmitters during that time. To be classified as stationary (i.e., consumed and excreted) during mobile tracking, transmitters had to be both (1) relocated on more than one occasion to ensure it had not moved and (2) never heard on any receivers further along the migratory route. A stationary transmitter was considered to be associated with the HCB if it was located at a tracking station within 3 km of the bridge structure.

To quantitatively identify stationary transmitters at the HCB, we fit a bivariate normal mixed model to square-root transformed continuous HCB time statistics for each transmitter detected at the HCB to distinguish between transmitters in live steelhead and transmitters continually pinging within range of HCB receivers. Long HCB time was indicative of a mortality, either consumed and detected while in a predator digestive tract (see below) or stationary, while short HCB time represented transmitters in live smolts, but may also represent transmitters consumed by a predator that quickly left the area and subsequently deposited on land or at an unmonitored marine location. The R package "mixtools" (Benaglia et al., 2009) was used to fit the model and estimate the parameters of the two distributions each year (e.g., Romine et al., 2014; Appendix S2: Figure S1). We calculated the probability that the HCB time statistic for each transmitter fit within the long HCB time distribution to quantitatively classify each transmitter as either being consumed ($p[x] > 0.95$) or not ($p[x] \leq 0.95$). Many of the transmitters identified as stationary based on length of time detected were also classified as stationary using mobile tracking methods. Data from the two independent methods provided additional confirmation and compensated for imperfect detection ability of the alternate method.

Locations of stationary transmitters were resolved when more than 1000 detections were recorded repeatedly in the same place without subsequent detection elsewhere. We used the point of highest density of the spatial distribution to pinpoint the location of the stationary transmitter. When the transmitter was located using mobile tracking only, we used the location of the station where the loudest (highest dB) detections were heard.

Density

Density plots for all survivors and all mortalities were executed with the Point Density tool in ArcMap using VPS positions. The density tool divided the number of detections around each raster cell by the specified surrounding area (circle with radius = 50 m) then plotted the values to create a density surface. To avoid pseudoreplication, position data were inversely weighted by number of detections per transmitter so that the output density value reflected the number of fish (or predators), rather than the number of detections, per square kilometer. Stationary transmitter detections were removed from the datasets prior to density calculation.

Hood Canal Bridge crossing

The location and mode of HCB crossing (around east drawspan, around west drawspan, or under pontoons) was described for each surviving smolt if a VPS positions on the south side of the HCB followed by a position on the north side were observed within 20 min, though the time elapsed between positions was typically much shorter ($\text{median}_{2017} = 2.5$ min, $\text{median}_{2018} = 3.3$ min). The location of crossing was the point at which the line between south and north positions crossed the midline of the HCB. The approximate time of crossing was determined by dividing the difference between the time of south position and time of north position by two, then adding the quotient to the time of south detection. If the crossing location was located within the open approach spans, we categorized the crossing route as "around," and if the crossing location occurred along the length of the HCB pontoons, we assumed the smolt navigated "under." We then paired the time of crossing with NOAA current velocity data and light level (day or night based on sunrise and sunset) to investigate factors that may affect crossing success. We used χ^2 goodness-of-fit tests on data from each year to determine whether smolts had a preference for crossing through the approach span rather than under pontoons, and whether smolts preferred to cross during day or night light conditions. To identify any smolt preference for crossing during certain tidal conditions, current velocity at each time of crossing was compared to mean daily current velocity using a paired t test.

Depth and temperature sensing transmitter

Recorded depths from 31 V9P (2017) and 31 V7P (2018) depth sensors, and temperature profiles from 34 V7T (2018) sensors detected at the HCB were used to provide a more detailed quantification of smolt behavior and identify predation events. For smolts with depth transmitters, we created a depth profile for each pressure sensor, then quantified the number of dives per hour, dive depth range, and max dive depth. We only quantified behavior during time segments where sequential detections were less than 10 min apart. A dive was defined as an increase in depth from the surface (depth < 2) to 3 m or more, followed by a return to the surface. Dive frequency was considered a minimum value because the transmitter ping rate was infrequent enough (30–90 s) that some short dives may have gone undetected. We identified abrupt changes in diving behavior that occurred only in transmitters classified as mortalities. Depth profiles of transmitters in smolt survivors exhibited nearly exclusive surface-oriented behavior, sometimes periodically interrupted by one or two short, shallow (<16 m) dives that often corresponded with HCB crossing times. In contrast, mortality profiles featured short time periods of surface residence, while the transmitter was presumably still in a smolt, followed by frequent deep dives. Departures from typical tagged fish behavior are commonly used to identify predation events (e.g., Gibson et al., 2015; Romine et al., 2014; Thorstad et al., 2011).

Locating predation events

The time of detection after a transmitter transitioned from continuous surface depth records (less than or equal to 2 m) to depths greater than or equal to 3 m was considered the time of a predation event. For temperature transmitters, we defined the time of predation as the first detection associated with a temperature increase that eventually rose to 35°C (maximum sensor value), with the assumption that a temperature increase of this magnitude meant the smolt had been eaten by a warm-blooded predator. We defined the location of predation as the VPS position triangulated closest in time (Δ_{time} < 21 min, median time = 4.7 min) to the time of predation. Spatial error around the predation location was calculated by multiplying the average speed of the transmitter movement within 1 h after the putative predation event by the time between the behavioral shift or temperature increase and the closest VPS position.

RESULTS

Survival probability estimates

Survival probabilities (±95% confidence interval) from release to RM were high in both years ($\phi_{REL-RM,2017}$ = 0.93 [0.85, 0.97]; $\phi_{REL-RM,2018(BBC)}$ = 0.98 [0.94, 0.99]; and $\phi_{REL-RM,2018(Skokomish)}$ = 0.92 [0.85, 0.96]). RM-HCB survival probabilities varied between years and between populations in 2018 ($\phi_{RM-HCB,2017}$ = 0.72 [0.65, 0.79]; $\phi_{RM-HCB,2018(BBC)}$ = 0.86 [0.80, 0.91], and $\phi_{RM-HCB,2018(Skokomish)}$ = 0.51 [0.41, 0.61]. Only about half of the steelhead detected at the HCB array survived past the bridge area to the TS array ($\phi_{HCB-TS,2017}$ = 0.49 [0.40, 0.58]; $\phi_{HCB-TS,2018}$ = 0.56 [0.48, 0.65]; Figure 3. In 2017, 63 smolts were classified as survivors and 68 classified as mortalities, and 86 smolts were classified as survivors and 83 classified as mortalities in 2018. Overall survival probability from RM to the JDF was 0.13 (0.06, 0.24) for both populations in 2017 and 0.13 (0.07, 0.22) (BBC) and 0.08 (0.04, 0.15) (Skokomish) in 2018. Detection probability of all receiver arrays exceeded 0.94, except for the array deployed in 2017 at the Skokomish RM (p = 0.45 [0.34, 0.56]; Appendix S1: Figure S1).

In 2017, Phase 1 of mark–recapture model comparison indicated no differences in ϕ_{REL-RM} or ϕ_{RM-HCB} by population, and a difference in detection probability p at each RM (Table 2). Models including separate estimates of ϕ_{REL-RM} or ϕ_{RM-HCB} by population had similar

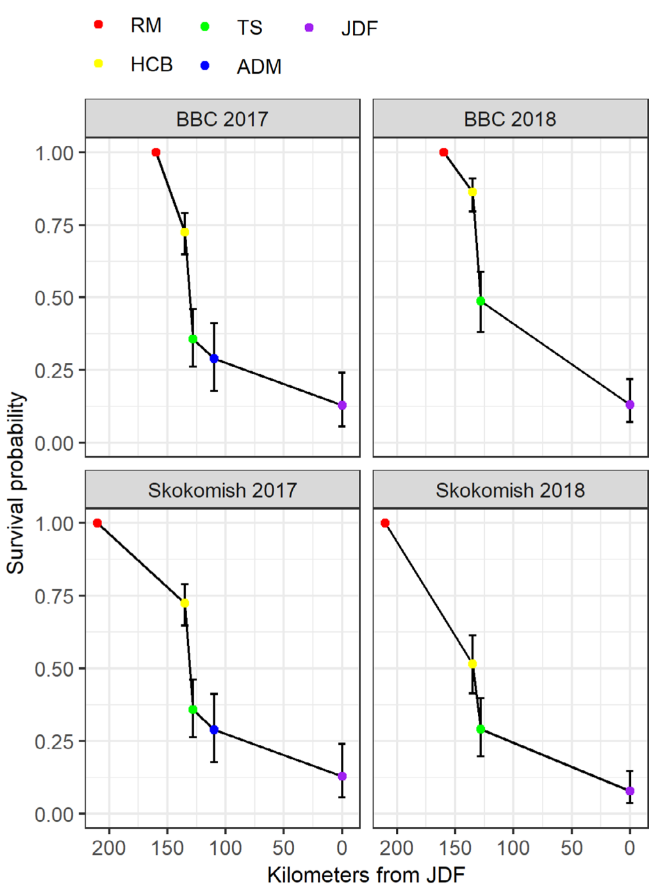

FIGURE 3 Cumulative survival (±95% confidence intervals) of tagged Big Beef Creek (BBC) and Skokomish River steelhead smolts from river mouth (RM; 160 and 210 km from final array, respectively) through acoustic arrays at the Hood Canal Bridge (HCB), Twin Spits (TS), and Admiralty Inlet (ADM), to the final array at the Strait of Juan de Fuca (JDF) in 2017 and 2018

support ($\Delta QAIC_c$ = 1.10 and 1.20, respectively) but had more parameters. Tag effects on *p* were only included in models with $\Delta QAIC_c$ greater than 2 (Table 2). For 2018 data, the model with the best fit estimated separate ϕ by population for both ϕ_{REL-RM} and ϕ_{RM-HCB}, and one *p* for both RMs and all transmitter types (Table 3), though models including separate estimates of ϕ_{RM-HCB} only and separate *p* at each RM had nearly identical support (ΔAIC_c = 0.12 and 0.48, respectively), so separate estimates of ϕ_{REL-RM} were not well supported. As in 2017, tag type did not affect *p*; the variable appeared only in 2018 Phase 1 models with ΔAIC_c greater than 2 (Table 2).

The week during which smolts first encountered the HCB affected the odds of survival in both years; models including encounter week had more support than base models selected in Phase 1 ($\Delta QAIC_{c,2017}$ = 2.56; $\Delta AIC_{c,2018}$ = 10.04; Tables 2 and 3). Weekly ϕ generally increased during later weeks of the smolts migration in both 2017 and 2018, though estimates of ϕ were more variable in 2018 (Figure 4). Neither approach location, diurnal phase, current velocity, tidal phase, body length, nor population variables improved model fit relative to the base model in 2017 ($\Delta QAIC_c > 3.17$; Table 2). A weak negative effect of body length (β = −0.02) was supported by the data in 2018 (ΔAIC_c = 6.75; Table 3), indicating lower probability of survival for smolts with longer fork length relative to survival of smaller smolts. AIC_c for models including all other Phase 2 variables were greater than AIC_c for the base model selected in Phase 1 ($\Delta AIC_c > 0.08$) and had at least one extra parameter (Table 3). All ϕ and *p* values were derived from the best fit model (Tables 2 and 3), except when we modeled approach week as a numeric variable to obtain a single ϕ_{HCB-TS} rather than weekly ϕs.

TABLE 2 The 2017 Cormack–Jolly–Seber (CJS) model results

Model	β	*K*	$QAIC_c$	$\Delta QAIC_c$	w_i
Phase 1					
ϕ (~segment)*p*(~array + a2:pop)		11	636.97	0.00	0.33
ϕ (~segment + s1:pop)*p*(~array + a2:pop)		13	638.07	1.10	0.19
ϕ (~segment + s2:pop)*p*(~array + a2:pop)		13	638.17	1.20	0.18
ϕ (~segment)*p*(~array + a2:pop + tagtype)		12	639.00	2.03	0.12
ϕ (~segment + s1:pop)*p*(~array + a2:pop + tagtype)		14	640.04	3.07	0.07
ϕ (~segment + s2:pop)*p*(~array + a2:pop + tagtype)		14	640.23	3.26	0.06
ϕ (~segment + s1:pop + s2:pop)*p*(~array + a2:pop)		15	641.51	4.54	0.03
ϕ (~segment + s1:pop + s2:pop)*p*(~array + a2:pop + tagtype)		16	643.53	6.56	0.01
ϕ (~segment + s1:pop)*p*(~array)		11	679.63	42.66	0.00
ϕ (~segment + s1:pop + s2:pop)*p*(~array)		13	683.41	46.44	0.00
ϕ (~segment)*p*(~array)		9	691.44	54.47	0.00
ϕ (~segment + s2:pop)*p*(~array)		11	695.39	58.42	0.00
Phase 2					
ϕ (~segment + s3:week)	−1.43 (16) – 1.08 (19)	20	634.41	0.00	0.53
ϕ (~segment)	…	11	636.97	2.56	0.15
ϕ (~segment + s3:length)	−0.01	12	637.59	3.17	0.11
ϕ (~segment + velocity)	−0.0004	12	638.65	4.24	0.06
ϕ (~segment + s3:day.night)	0.13 (day)	13	639.06	4.64	0.05
ϕ (~segment + s3:side.mid)	0.26 (side)	13	640.24	5.82	0.03
ϕ (~segment + s3:tag)	0.11 (V8)	13	640.49	6.08	0.03
ϕ (~segment + s3:tide)	−0.10 (ebb)	13	641.07	6.66	0.02
ϕ (~segment + s3:population)	−0.03 (BBC)	13	641.15	6.74	0.02

Notes: Survival probability (ϕ) and detection probability (*p*) were modeled in two phases. Segment refers to migration segment (s1 = release-river mouth [RM] segment, s2 = RM-Hood Canal Bridge segment); array refers to receiver array (a2 = RM array; pop = population). Model structure, number of parameters (*K*), quasi-likelihood Akaike information criteria ($QAIC_c$), $\Delta QAIC_c$, and model weight (w_i), and the beta estimate (β) and factor level for each predictor variable in Phase 2 models are listed. All Phase 2 models allowed *p* to vary at each array and at each RM (see text for explanation of variables).

TABLE 3 The 2018 Cormack–Jolly–Seber (CJS) model results

Model	β	*K*	AIC_c	ΔAIC_c	w_i
Phase 1					
ϕ (~segment + s1:pop + s2:pop)*p*(~array)		11	723.70	0.00	0.23
ϕ (~segment + s2:pop)*p*(~array + a2:pop)		11	723.82	0.12	0.21
ϕ (~segment + s2:pop)*p*(~array)		9	724.17	0.48	0.18
ϕ (~segment + s2:pop)*p*(~array + a2:pop + tagtype)		12	725.85	2.15	0.08
ϕ (~segment + s1:pop + s2:pop)*p*(~array + a2:pop + tagtype)		14	725.94	2.24	0.07
ϕ (~segment + s1:pop)*p*(~array)		9	753.84	30.15	0.00
ϕ (~segment)*p*(~array)		7	754.69	30.99	0.00
ϕ (~segment + s1:pop)*p*(~array + a2:pop)		11	756.06	32.36	0.00
ϕ (~segment)*p*(~array + a2:pop)		9	756.13	32.44	0.00
ϕ (~segment + s1:pop)*p*(~array + a2:pop + tagtype)		12	756.38	32.68	0.00
ϕ (~segment)*p*(~array + a2:pop + tagtype)		10	756.83	33.13	0.00
Phase 2					
ϕ (~segment + s1:pop + s2:pop + s3:week)	-1.79 (19) - 1.88 (22)	21	713.65	0.00	0.92
ϕ (~segment + s1:pop + s2:pop + s3:length)	−0.02	12	718.95	5.30	0.06
ϕ (~segment + s1:pop + s2:pop)	...	11	723.70	10.04	0.01
ϕ (~segment + s1:pop + s2:pop + s3:velocity)	−0.01	12	723.78	10.13	0.01
ϕ (~segment + s1:pop + s2:pop + s3:pop)	−0.24 (BBC)	13	724.23	10.58	0.00
ϕ (~segment + s1:pop + s2:pop + tagtype)	0.03 (V8)	13	727.23	13.58	0.00
ϕ (~segment + s1:pop + s2:pop + s3:side.middle)	0.21 (side)	13	727.56	13.91	0.00
ϕ (~segment + s1:pop + s2:pop + s3:tide)	0.15 (ebb)	13	727.80	14.15	0.00
ϕ (~segment + s1:pop + s2:pop + s3:day.night)	0.05 (day)	13	727.82	14.17	0.00

Note: Survival probability (ϕ) and detection probability (*p*) were modeled in two phases. Segment refers to migration segment (s1 = release-river mouth [RM] segment; s2 = RM-Hood Canal Bridge segment); array refers to receiver array (a2 = RM array; pop = population). Model structure, number of parameters (*K*), Akaike information criteria (AIC_c), delta AIC_c, and model weight (w_i), and the beta estimate (β) and reference level for each predictor variable in Phase 2 models are listed. All Phase 2 models allowed *p* to vary at each array and at each RM (see text for explanation of variables).

Travel and HCB time

Survivors spent an average of 1.9 (±SE 0.6) days in 2017 and 0.9 (±SE 0.2) days in 2018 within range (~400–500 m on either side) of the HCB, while only taking an average of 0.2 (±0.02) and 0.3 (±0.03) days, respectively, to travel the subsequent 7-km migration segment from HCB-TS (Figure 5). Transmitters categorized as mortalities were detected for an average of 44.2 (±5.2) days in 2017 and 35.3 days in 2018 within range of the HCB (truncated by battery limitation). The entire marine migration from RM-JDF took Big Beef Creek smolts an average of 17.1 days in 2017 and 12.6 days in 2018, while Skokomish smolts took an average of 15.8 days in 2017 and 14.2 days in 2018 (Figure 5).

Stationary transmitters

In 2017, we detected 35 stationary transmitters via mobile tracking, 33 of which were within 3 km of the HCB. The two other stationary transmitters were detected between the HCB and TS (5.5 and 6 km north of the HCB; Appendix S3: Figure S1). In 2018, we detected 19 stationary transmitters, all of which were located within 3 km of the HCB except for one transmitter found in south Port Gamble Bay (Appendix S3: Figure S1). Several stationary transmitters identified by mobile tracking were also determined to be stationary using mixed model analysis of fixed array detections. Using both methods, 49 (78% of mortalities) of the smolts detected at the HCB were stationary in 2017, and 47 (57% of mortalities) were stationary in 2018.

Stationary transmitter locations were concentrated near the HCB and less likely to be found at stations father away from the structure. Locations were distributed along the entire length of the HCB, but a higher density was observed along the western portion, especially in 2018 (Appendix S3: Figure S1). Three stationary transmitters were found each year in Port Gamble Bay, near documented harbor seal haulouts (Jeffries

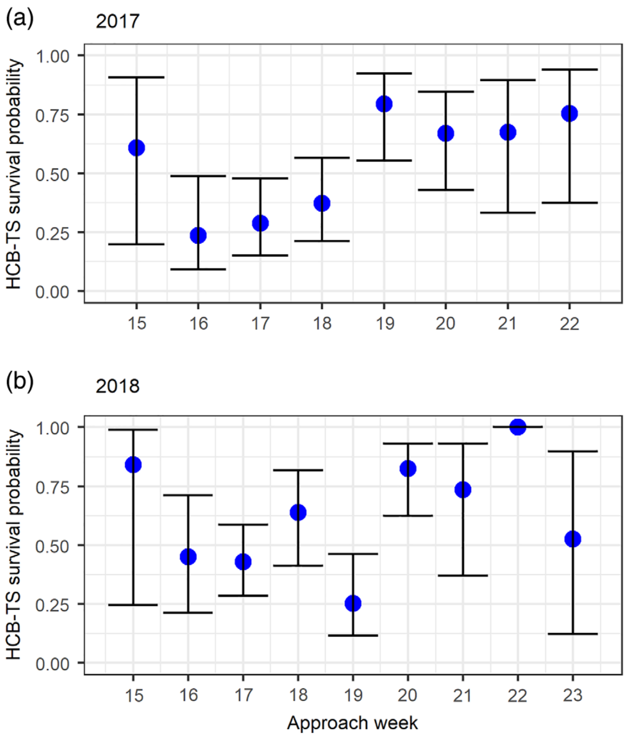

FIGURE 4 Steelhead smolt survival probabilities (±95% confidence intervals) from the detection at the Hood Canal Bridge (HCB) to the Twin Spits array (TS) by approach week in 2017 (a) and 2018 (b)

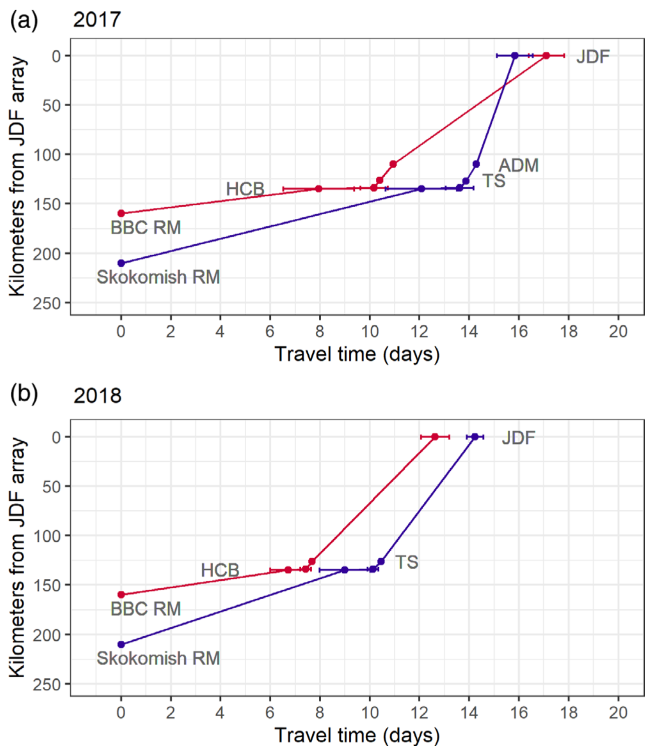

FIGURE 5 Average travel time in days (±SE) of Skokomish (SKOK; blue line) or Big Beef Creek (BBC; red line) steelhead smolts detected moving from the river mouth (RM) to the Hood Canal Bridge (HCB), the Twin Spits array (TS), Admiralty Inlet (ADM; 2017 only), and the Strait of Juan de Fuca (JDF) in 2017 (a) and 2018 (b), plotted in relation to the distance of each detection point to the JDF array

et al., 2003), in addition to transmitters deposited on the route from HCB to Port Gamble Bay (Appendix S3: Figure S1).

Density

Smolt density patterns of survivors near the HCB were similar in 2017 and 2018. Densities were higher on the south side of the HCB and near the corners formed by the cross-pontoons. Survivors were also more often located on the east side of the HCB compared to the west side. Particularly in 2017, high densities of survivors were located in the open areas under the east and west approach spans (Figure 2) more often than along adjacent bridge spans (Figure 6).

Density patterns of mortalities were also similar in both study years. Similar to survivors, mortalities were concentrated along the south side of the HCB and also tended to spend time in corner areas formed by perpendicular pontoons (Figure 2), but were located near the center drawspan less frequently than survivors (Figure 6). Mortalities were more uniformly distributed across the length of the HCB than survivors (Figure 6), but this could be attributed to the difference in number of observations; many more positions were resolved for mortalities (2017: 18,492; 2018: 28,795, excluding detections of transmitters that became stationary) than for survivors (2017: 3272; 2018: 3173).

Crossing locations

Out of 41 crossing events documented in 2017, 13 (32%) smolts crossed under the east approach, seven (17%) crossed under the west approach, and 21 (51%) were determined to have crossed under the pontoons (Figure 7). In 2018, a higher percentage of smolts crossed under the HCB than in 2017, with 52 (77%) smolts crossing under, and only nine (13%) crossing the east and seven (10%) crossing under the west approach. All but one smolt detected crossing the bridge survived to TS or ADM. Smolts were more likely to cross under the approach spans than they were to cross under the pontoons ($\chi^2_{2017} = 43.105$, $p < 0.001$; $\chi^2_{2018} = 12.444$, $p < 0.001$). Smolts that crossed under the pontoons did not appear to have a preference for certain crossing locations, rather the crossings were distributed somewhat evenly along the length of the HCB. Crossing location distribution was similar between years, except that

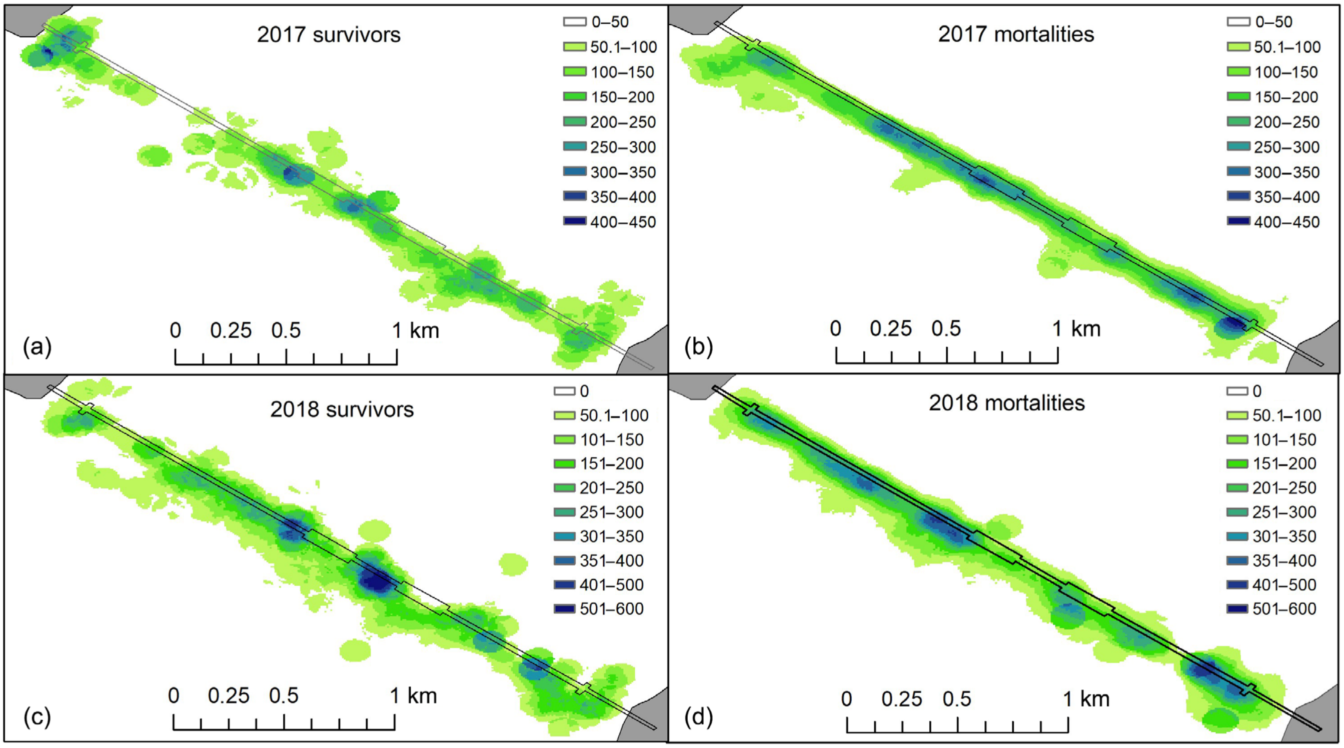

FIGURE 6 Density plots, inversely weighted by number of detections per fish, showing the density of VPS positions of tagged smolts encountering the Hood Canal Bridge (HCB) that survived to the TS array or beyond ("survivors") in 2017 (a), positions of tags not detected after the HCB ("mortalities") in 2017 (b), survivors in 2018 (c), and mortalities in 2018 (d). Density values are in smolt positions per square kilometer and scale by sample size

11 smolts crossed under the center drawspan in 2018, whereas only one smolt crossed at that location in 2017 (Figure 7). In 2017, crossing events took place in proportion to the number of day and night time hours ($\chi^2 = 0.000$, df $= 1$, $p = 0.984$), whereas smolts showed a preference for crossing during daylight hours in 2018 ($\chi^2 = 19.892$, df $= 1$, $p < 0.001$). Most smolts that crossed under the bridge did so during morning daylight hours, but no temporal pattern emerged for smolts crossing around (Figure 7). Crossing events were much more likely to occur during ebb tides when currents were moving in the same direction as the smolt migration ($t_{2017} = 10.995$, df $= 54$, $p < 0.001$; $t_{2018} = 16.954$, df $= 67$, $p < 0.001$; Figure 8). In 2018, crossing events appeared to occur more frequently when current velocities were greater (Figure 8).

Depth distribution and evidence of predation

In 2017, 31 smolts implanted with pressure-sensing transmitters were detected at the HCB. In total, 13 survived to TS, and 18 did not. All 13 survivors exhibited strong surface orientation. Ninety-one percent of detections indicated migration in the top 1 m of the water column, and 95% in the top 3 m (Table 4). Subsequently, all 13 survivors migrated past the TS array at average depths less than 1 m. Seven of the 13 survivors were initially recorded at the surface, then exhibited one to three short shallow dives per smolt before returning to depths less than 1 m (e.g., Figure 9a, Table 5). The remaining six survivors remained exclusively within the top 2 m while within range of the HCB array.

For the 18 mortalities with depth sensors in 2017, only 38% of detections occurred in the top 1 m and 45% in the top 3 m (Table 4). In all, 15 of the 18 mortalities were initially detected near the HCB at depths less than 1 m (exhibiting behavior typical of a live smolt), then subsequently exhibited frequent dives (e.g., Figure 9b, Table 5). We infer that the 15 mortalities exhibiting the diving behavior were consumed by predators because no surviving smolts exhibited this behavior and because it is characteristic of marine mammals and some diving birds. Six of those 15 mortalities were subsequently detected stationary by the HCB array (e.g., Figure 9c). In all, 15 of 18 mortalities dove to 38 m at least once (Table 5). A single mortality exhibited frequent diving behavior (7.5 dives/h) to intermediate depths (max $= 25$ m), then was last detected near the surface. Time between first detection at the HCB and the 15 predation events averaged

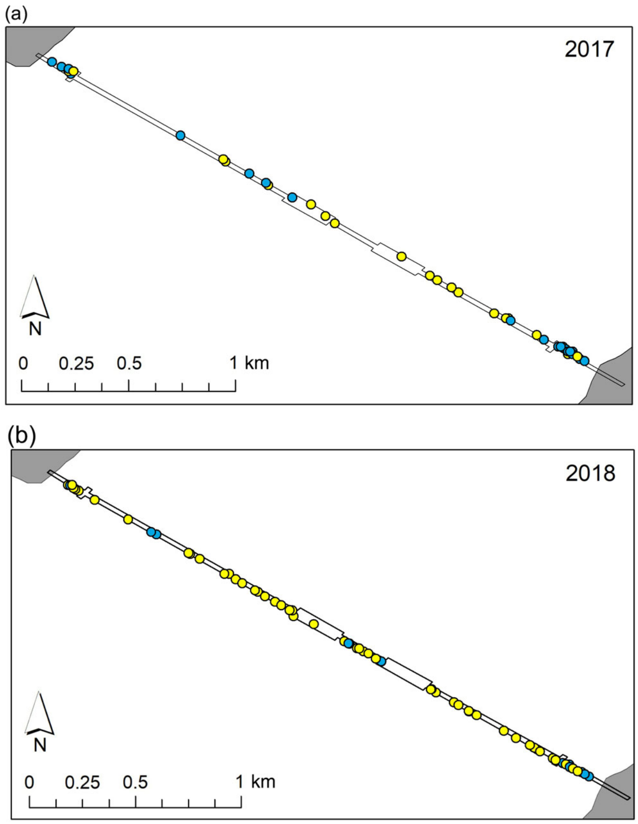

FIGURE 7 Locations of where tagged steelhead smolts crossed from the south to the north side of the Hood Canal Bridge in 2017 (a) and 2018 (b). Yellow points represent crossings that took place between sunrise and sunset (day), while blue circles represent crossings between sunset and sunrise (night)

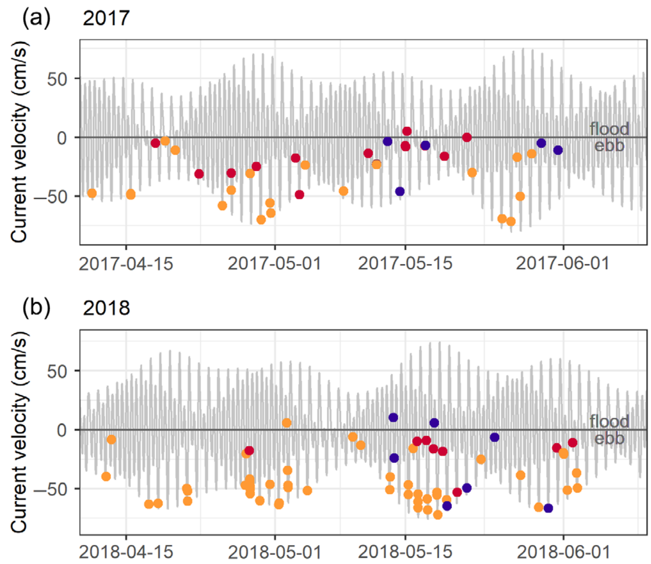

FIGURE 8 Precise Hood Canal Bridge crossing time of smolts that crossed under (orange points), around through the east approach span (red points), or around through the west approach span (blue points) in 2017 (a) and 2018 (b) in relation to current velocity (predictions at NOAA current station PUG1603, https://tidesandcurrents.noaa.gov/noaacurrents/Predictions?id=PUG1603_20). Currents indicative of flood tides are represented using positive values, while currents during ebb tides are represented by negative values

16.7 h, with five of the 18 events occurring within 1 h after first detection at the HCB, and all predation events within 2 days after first detection at the HCB.

In 2018, depth sensor data for 19 survivors and 13 mortalities detected at the HCB revealed behavioral patterns similar to those observed in 2017. At the HCB, most detections of survivors (82%) occurred at depths in the top meter of the water column and 87% in the top 3 m (Table 4). Nearly all survivors (95%) in 2018 migrated past the TS array in average water depths less than 1 m. At the HCB, mortalities were located in the top meter only 30% of the time and 28% in the top 3 m (stationary transmitters excluded) in 2018 (Table 4). Four of the 19 survivors remained at depths less than 2 m as they migrated past the HCB, while the remaining 15 surviving smolts exhibited short dives as they passed the HCB (e.g., Figure 9a, Table 5). Similar to 2017, most smolts that were eventually determined to be mortalities (11 of 13) approached the bridge near the surface (≤2 m) and subsequently exhibited frequent deep dives, each with at least one dive greater than 37 m (e.g., Figure 9b, Table 5). Six of these 11 frequent deep divers was subsequently found to be stationary (e.g., Figure 9c). One of the 13 mortalities exhibited shallower dives ($\bar{x}$ = 3.8 m, max = 17 m) occurring much more frequently (11.5 dives/h) than the other 2018 mortalities, and was not found stationary within our monitoring network. Most predation events (nine of 12) occurred in less than 6 h ($\bar{x}$ = 1.6) from the time of initial detection at the HCB, while the remaining three events occurred within 36–243 h. One final 2018 mortality did not display a behavioral pattern consistent with predation, but remained nearly exclusively in the top 2 m (one detection at 3.1 m), indicating that the assumed mortality event took place outside the detection range of the HCB array.

Temperature changes and evidence of predation

In all, 11 of the 16 temperature sensors in 2018 non-surviving steelhead exhibited temperature profiles consistent with being consumed by a warm-blooded predator. These 11 transmitters were initially detected on the HCB array in ambient temperatures (9–14°C), then recorded for a period of time (1.5–81.5 h) at 35°C before either exiting receiver range or abruptly returning to ambient

TABLE 4 Distribution of depth transmitter records for survivors and mortalities

Depth (m)	2017 No. survivor detections	2017 Mortality detections *N*	2017 Mortality detections Proportion mortalities	2018 No. survivor detections	2018 Mortality detections *N*	2018 Mortality detections Proportion mortalities
0–1	3806	8007	0.68	3198	7944	0.71
2	119	644	0.84	158	1253	0.89
3	47	861	0.95	38	842	0.96
4–10	189	7588	0.96	379	11,322	0.97
11–16	37	935	0.96	63	2197	0.97
16–34	0	1556	1.0	50	2244	0.98
35–38	0	1740	1.0	0	663	1.0

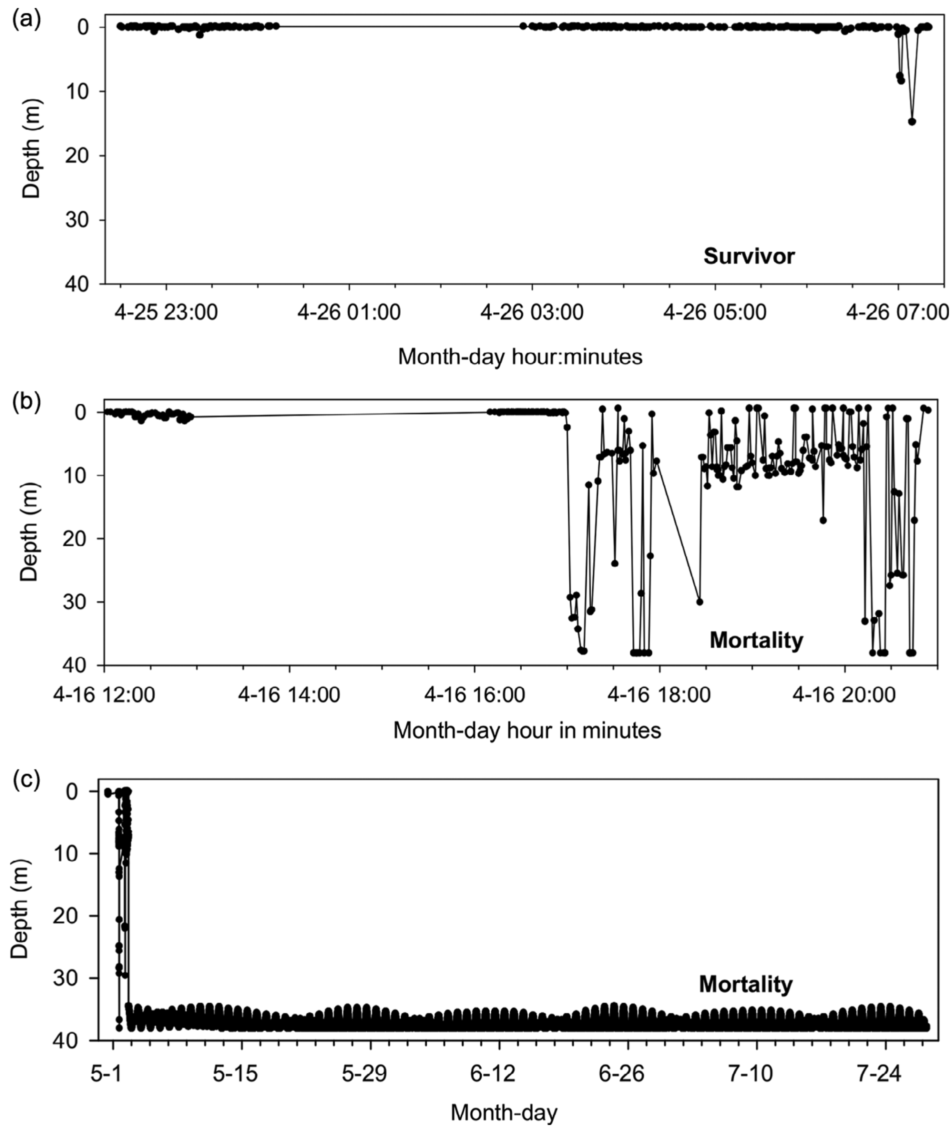

FIGURE 9 Depth profiles of steelhead smolts exhibiting behavior typical of a surviving smolt (a), a non-surviving smolt that was eaten by a deep and frequently diving predator (b), and a non-surviving smolt that was eaten then deposited by a predator to become stationary until the transmitter battery expired (c). The maximum value of the depth sensors was 38 m

TABLE 5 Depth sensor summary

Year and fate of transmitter	N	Hours of behavior sampled	No. dives/hour (mean ± SE)	Dive depth maximum	No. tags recording >37-m depth
2017 survivors	13	40	0.4 ± 0.1	16.5	0
2017 mortalities	18	104	4.5 ± 0.6	38.0[a]	15
2018 survivors	19	40	1.1 ± 0.2	24.8	0
2018 mortalities	13	122	4.6 ± 0.2	38.0[a]	11

[a]Sensor maximum.

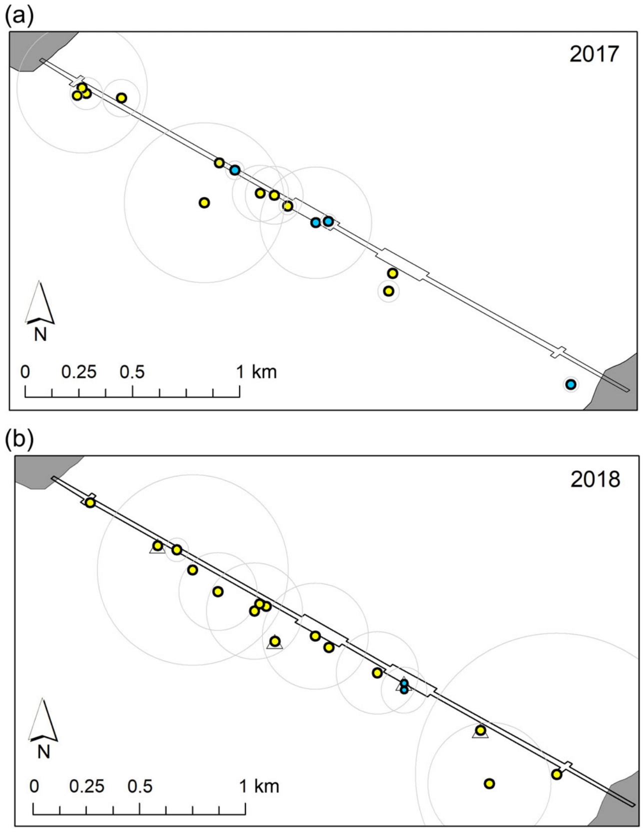

FIGURE 10 Locations of predation events inferred by changes in diving behavior or increases in transmitter temperature in 2017 (a) and 2018 (b). Yellow points represent predation events that occurred during day hours, while blue points depict events that occurred during the night. Gray circles around most symbols represent the error radius in meters (some are so small they are obscured by the symbol), with triangles surrounding points where data were not available for error calculation

temperature. Six of the 11 sensors with elevated temperature were detected within range of Sisters Rock, a known harbor seal haulout 750 m south of the HCB, and seven of the 11 warm sensors were found stationary within the range of our sampling area. The temperature increase occurred an average of 17.9 h after arrival at the HCB (four of 11 events occurred after <1 h). The temperature sensors in the remaining five mortalities showed no sign of abnormal temperature increase and were not detected as stationary.

We were able to establish the predation location of 15 of 16 (2017) and seven of 12 (2018) non-surviving depth-tagged smolts, and 10 of the 11 transmitters that exhibited temperature increase (the remaining mortalities did not have a VPS location within 20 min of the change in diving behavior/temperature). Predation locations in both study years tended to be closer to the HCB rather than further toward the edge of detection range, and were somewhat spread out, with a slightly western bias, along the bridge length (Figure 10). Numerous predation events (13 of 32) over both years took place in close proximity to the corners formed by the perpendicular pontoons' intersection with the main bridge pontoons (Figure 2), and one event appears to have occurred in the west pool (Figure 10a).

DISCUSSION

In both years of this study, approximately half of all steelhead smolts approaching the HCB died while attempting passage or soon after. This study estimated survival probabilities from RM to the Strait of JDF ranging from 8% to 13%, so removing HCB associated mortality could theoretically increase early marine survival to 16%–26%. Life cycle modeling parameterized using metrics specific to Puget Sound steelhead populations concluded that early marine survival rates need to exceed 14%–16% to achieve positive population growth (National Marine Fisheries Service, 2019). The HCB mortality at the levels estimated in this study put early marine survival below that level. Even though many factors are likely to affect early marine survival of steelhead in Hood Canal, including environmental variation and ecological interactions with other species (e.g., Moore et al., 2021), this study suggests that the HCB is an important source of mortality.

The HCB negatively affects steelhead and likely many other mobile species that move between Hood Canal and the main Puget Sound basin. Steelhead smolts slowed considerably upon approaching and attempting to pass the bridge, taking 1–2 days on average to navigate past the bridge compared to just 5–7 h to travel the subsequent 7 km to the TS array. Hydrodynamic modeling of the near-field effects of the HCB indicates the disruption of surface currents and changes in temperature and salinity that are most severe at the bridge, but extend up to 2–3 km away (Khangaonkar et al., 2018). These effects are likely contributing to delay and alteration of migration behavior, as salmon smolts are known to use environmental cues to guide migration in marine waters (Burke et al., 2013; Healey & Groot, 1987; Thorstad et al., 2012).

The delays observed at the HCB may also be a result of steelhead smolts engaging in anti-predator behaviors like slowing, avoiding, or evading in response to the presence of predators. Anthropogenic structures can change the predator–prey dynamics of a system, creating foraging habitat that favors the predator, and increasing predation risk for migrating species (Sabal et al., 2021). For example, lights illuminating a bridge crossing the Puntledge River in British Columbia, Canada, also illuminated portions of the river adjacent to the bridge, allowing predators to easily spot the silhouettes of migrating salmon (Yurk & Trites, 2000). Alcott et al. (2020) found that snapping turtles (*Chelydra serpentina*) took advantage of slower movement rates and higher densities of migrating river herring at road-crossing culverts where stream width was constricted. Steelhead typically migrate quickly through Puget Sound (Moore et al., 2015), and reductions in their typically rapid pace at the HCB are likely to increase susceptibility to predation because they spend more time navigating and are forced to take a tortuous rather than linear path. Theoretically, the predation risk of migrating prey increases with time exposed to predators (Peterson & DeAngelis, 2000). Though we cannot disentangle the effects of migration delay and effects of the HCB structure itself, because every tagged smolt experiences both, we do consistently see increased mortality near the bridge where migration slows, relative to other receiver arrays where migration is unrestricted (Moore & Berejikian, 2013).

Predation was likely the primary cause of mortality for steelhead smolts at the HCB. Stationary transmitters were much more frequently located near the bridge than farther away. The spatial distribution of stationary transmitters all along the HCB suggests that predators ingested tagged smolts and either regurgitated or digested and defecated transmitters onto the seafloor. Prolonged immobilization at one location is not a behavior observed in steelhead, and interpreting stationary transmitters as mortalities due to predation has been widely adopted (Klinard & Matley, 2020). This assumption is further substantiated by the spatial density analysis, which showed high densities of mortalities (transmitters that were still mobile yet were not detected at TS or beyond) near the HCB in both years. High densities of mortalities indicate that predators eating steelhead at the HCB were foraging regularly at that location rather than opportunistically encountering prey as they migrated through the area. Stationary transmitters were also found near Port Gamble Bay and Sisters Rock, which are known harbor seal haulouts (Figure 1; Jeffries et al., 2003), as well as along the routes from the HCB to the haulouts, implicating harbor seals as a likely predator species.

Several predator species were observed in high abundance in the vicinity of the HCB during steelhead migration (Stocking & Pearson, 2019). Transmitter depth, temperature, and movement patterns combined strongly suggest that harbor seals were the predominant predator of steelhead in this study. First, data from steelhead implanted with temperature sensors showed that a majority of the transmitters consumed reached 35 degrees, ruling out ectotherms and leaving birds and marine mammals as potential predators. Second, dive data from the depth sensors confirmed not only that the majority of transmitters consumed exhibited similar behavior, but the depth, magnitude, and frequency of dives ruled out the more abundant bird species observed at the HCB. For example, pigeon guillemots (*Cepphus columba*), the most abundant avian species in both years, exhibited density patterns suggesting a preference for the HCB, yet do not typically dive to depths greater than 20 m (Stocking & Pearson, 2019), whereas nearly all consumed depth sensors in steelhead (84%) logged depths at or near the maximum 38 m. Finally, the high density of non-survivor positions and stationary transmitters at the HCB (Figures 6 and 7) suggests a resident predator rather than a transient species. The only marine mammals consistently observed at the HCB in April and May were harbor seals and harbor porpoise (*Phocoena phocoena*; Stocking & Pearson, 2019), and anecdotal inter-species comparison of foraging behavior in the immediate vicinity of the HCB suggests that harbor seals are much more likely than harbor porpoise to exhibit localized foraging patterns (Port Gamble S'Klallam Tribe, 2021).

Harbor seals are abundant in Hood Canal, as they are in the whole of Puget Sound, where population levels were thought to have reached carrying capacity by the late 1990s (Jeffries et al., 2003), but may have increased in abundance since then (see Jefferson et al., 2021). Recent studies have documented the potential impact of harbor seal predation on salmonid species of conservation concern (Chasco et al., 2017; Thomas et al., 2016). The combination of telemetry and survey data suggests that Hood Canal harbor seals responded behaviorally and numerically to increased prey density at the HCB. Boat-based predator surveys observed higher densities of harbor seals within 300 m of the HCB relative to stratums further away in 2017 (though not in 2018; Stocking &

Pearson, 2019). Additional surveys conducted from the bridge deck in 2018 observed high densities of harbor seals near the bridge compared to distant areas (Port Gamble S'Klallam Tribe, 2021). In addition to increased numbers of predators, there appears to be an increase in the number of steelhead consumed by resident harbor seals in this area compared to other areas not impacted by submerged pontoons (see Moore & Berejikian, 2013). This impact may also apply to other ESA-listed species like Chinook salmon and chum salmon, though data are unavailable to assess altered behavior or predation impacts on other salmon at the HCB.

Inferred predation events occurred in close proximity to the HCB after variable amounts of time post-arrival. Steelhead smolts migrated through Hood Canal almost exclusively in the top 1–2 m of the water column, enabling a clear distinction between behaviors of live migrating smolts and smolts ingested by predators. This distinction, coupled with fine-scale positioning data, allowed for the identification of the precise time and location of 26 predation events over 2 years. In all, 11 additional predation events were identified in 2018 using the time of temperature sensor increase. Seventy-nine percent of the mortality between the HCB and TS was attributed to predation events occurring within 500 m of the HCB (approximate range of the hydrophone array). The remaining mortality may also have occurred near the HCB without being detected; for example, if predators consuming a tagged smolt left the array before behavioral patterns could be established. Some predation events occurred soon after smolts arrived at the HCB and others well after initial detection. All smolts were likely delayed to some degree; therefore, it is difficult to determine a precise relationship between delay time and risk of predation at the HCB.

The week steelhead smolts approached the HCB had the strongest effect on HCB-TS survival of all the variables we tested, and survival generally increased during the later weeks of the migration. Ecological changes during the spring months may influence how the HCB influences predator–prey interactions and the survival of steelhead and other salmon. An annual biomass influx, the release of hatchery salmon into Hood Canal, occurs just prior to steelhead smolt migration and may have contributed to the variability in predation rates we observed in 2017 and 2018. In early April, 25–32 million chum fry were released in South Hood Canal, followed by nearly one million coho in mid- to late-April and 6–7 million Chinook salmon (age 0 and age 1) from late April to late May (RMIS database; https://www.rmpc.org/, accessed November 2019). These species migrate at different rates and occupy different habitats, but in aggregate likely result in a major increase in the abundance of all salmonids at the HCB beginning sometime in May. Total abundance of these species of Pacific salmon would greatly outnumber the migrating wild steelhead and may provide alternative prey resources for those predators consuming steelhead smolts at the HCB. Prey switching by a primary predator can alleviate pressure on migrating fish when an alternate prey species is preferred or conditionally available (Moore et al., 2021; Wells et al., 2017). In the Fraser River, high densities of co-migrating conspecifics improved survival of sockeye salmon smolts (Furey et al., 2015), demonstrating the capacity of abundant prey to reduce individual predation risk.

Steelhead smolt body length at tagging also affected odds of survival past the HCB in 2018 (and marginally in 2017); longer smolts were less likely to survive to TS than shorter smolts. Larger size is generally thought to confer a survival advantage over smaller conspecifics due to decreased vulnerability to predation (Sogard, 1997), though size selectivity patterns can vary by predator species or habitat (Halfyard et al., 2012; Hostetter et al., 2012), or can shift over time (Ward, 2000). Size selectivity often occurs as a result of predator preference for one size of prey over another, where predators seek to maximize energy intake but may be limited by costs of pursuit or gape size, or where prey of certain sizes are more conspicuous (Sogard, 1997). Lower survival of larger smolts past the HCB is likely explained by harbor seals targeting large prey to maximize energetic gains. Harbor seals are large bodied and are not gape limited or likely to have difficulty capturing a 200-mm smolt, given their ability to consume much larger prey (Lance et al., 2012). Harbor seals can use their vibrissae (whiskers) to sense disruptions in water currents to locate and capture prey, and can differentiate between hydrodynamic trails left by objects of different sizes (Wieskotten et al., 2011). Therefore, stronger hydrodynamic signals left by larger smolts relative to signals created by smaller prey would make larger smolts easier to locate and pursue, and may explain or contribute to size selectivity at the HCB.

Unfortunately, the impact of the HCB on ESA-listed Chinook and chum salmon is not as readily measured as it has been for steelhead. Puget Sound steelhead smolts migrate rapidly in a directed manner, spending very little time in the early marine environment before reaching the Pacific Ocean (Moore et al., 2015). In contrast, Chinook, chum, and coho salmon display more variability in their migration behavior and tend to spend more time than steelhead in estuarine and nearshore habitats before exiting Puget Sound (Duffy et al., 2005; Quinn, 2005). Portions of Chinook and coho salmon populations may also reside in Puget Sound for the entire duration of marine life (Chamberlin et al., 2011; Simenstad et al., 1982). These behavioral characteristics make it difficult to quantify survival because there is no obvious spatial component of the migration route that temporally corresponds with migration success as there is with steelhead. However, it is likely that other salmon species are being impacted to some degree. Video data from the south side of the HCB show high densities of Chinook and chum salmon, in particular, swimming against the current alongside the pontoons (Port Gamble S'Klallam Tribe, 2021). Though it does not appear to be the case with steelhead, other juvenile fish may be attracted to the HCB, utilizing the structure for foraging opportunities provided by considerable marine growth. Increased feeding opportunities at the HCB may come at the cost of delayed migration and increased predation risk. Other unknown impacts include potential alterations to the migration behavior of adult salmonids.

Steelhead smolts were either less able or willing to cross under or around the HCB during flooding tidal conditions than during ebb tides. No crossings were detected during strong flood tides (Figure 9), which means that the temporal window for crossing is much shorter than it would be if the HCB was passable under all tidal conditions. Most smolts (>85% in both years) were first detected on the HCB array during ebb tides, so generally appear to be using outgoing currents to navigate out of Hood Canal. HCB passage only during ebb tides adds to the delay caused by physical properties of the bridge and effects on water currents. In our GLM analysis, tide direction at the time of arrival near the HCB was not an important indicator of survival past the HCB, so arriving during an ebb tide does not appear to infer a strong survival advantage, though the small number of smolts arriving during flooding tides may have prevented our ability to detect a tidal effect.

The majority of identified predation locations were within 100 m of the HCB and appeared biased toward the corners formed by the perpendicular pontoons extending from the east and west ends of the pontoons and from either side of the drawspan (Figure 10). Sonar data from spring of 2018 show harbor seals herding fish into these semi-enclosed corner areas (Port Gamble S'Klallam Tribe, 2021), likely a foraging strategy that utilizes the HCB to increase prey density and thus probability of capture. Eddies formed around these perpendicular pontoons may also be deterring migrating fish from locating the nearshore openings. Predation events occurred predominantly during daylight hours, suggesting that excess lighting on the HCB is not an important factor affecting predation dynamics. Future work should focus on bridge modifications that eliminate or fill corner areas to reduce prey entrapment and facilitate directional currents toward the open areas under the East and West approach spans.

Steelhead originating in Hood Canal rivers need continuous migration corridors to complete the marine phase of their life cycle. The HCB disrupts the ability of steelhead smolts to reach the Pacific Ocean and likely impacts other species of salmon as well. The findings add to a growing list of transportation infrastructure impacts on migratory animals (Sabal et al., 2021; Shepard et al., 2008; Wilcove & Wikelski, 2008), and provide detailed information for assessing future changes and modifications to the HCB to reduce migration delays and associated predation. Furthermore, the study highlights how understanding animal behavior, such as the strong surface orientation of steelhead smolts, can help to avoid unintended consequences of new or modified transportation infrastructure.

ACKNOWLEDGMENTS

This study was strongly supported through funding procurement (Salmon Recovery Funding Board and the State of Washington) and coordination work by Long Live the Kings, especially Iris Kemp, who also graciously handled permits for receiver deployment activities. Mike Haggerty (NOAA) queried RMIS for hatchery release information. Rob Endicott, Dan Lomax, Wes Parker, Sean Sol, Katy Doctor, Iris Kemp, Joy Lee, Mat Gillum, and Kevin Redman helped with trapping, tagging, mobile tracking and receiver rigging, deployment, and most importantly, retrieval. Thanks also goes to Dana Allen with InnovaSea Inc. for guidance and consulting on experimental and telemetry array design, and to Hans Daubenberger for helpful analysis at decision points throughout the study.

CONFLICT OF INTEREST

The authors declare no conflict of interest.

DATA AVAILABILITY STATEMENT

Data (Moore & Berejikian, 2022) are available from Dryad (https://doi.org/10.5061/dryad.8pk0p2npn).

REFERENCES

Alcott, D., L. Long, and T. Castro-Santos. 2020. "Wait and Snap: Eastern Snapping Turtles (*Chelydra serpentine*) Prey on Migratory Fish at Road-Stream Crossing Culverts." *Biology Letters* 16: 20200218.

Benaglia, T., D. Chauveau, D. R. Hunter, and D. Young. 2009. "mixtools: An R Package for Analyzing Finite Mixture Models." *Journal of Statistical Software* 32: 1–29.

Bestley, S., I. D. Jonsen, M. A. Hindell, C. Guinet, and J.-B. Charrassin. 2012. "Integrative Modeling of Animal Movement: Incorporating In Situ Habitat and Behavioural Information for a Migratory Marine Predator." *Proceedings of the Royal Society B* 280: 20122262.

Bulleri, F., and M. G. Chapman. 2010. "The Introduction of Coastal Infrastructure as a Driver of Change in the Marine Environment." *Journal of Applied Ecology* 47: 26–35.

Burke, B. J., M. C. Liermann, D. J. Teel, and J. J. Anderson. 2013. "Environmental and Geospatial Factors Drive Juvenile Chinook Salmon Distribution during Early Ocean Migration." *Canadian Journal of Fish and Aquatic Sciences* 70: 1167–77.

Burnham, K. P., D. R. Anderson, G. C. White, C. Brownie, and K. H. Pollock. 1987. *Design and Analysis Methods for Fish Survival Experiments Based on Release-Recapture*. American Fisheries Society Monograph 5. Bethesda, MD: American Fisheries Society.

Celedonia, M. T., R. A. Tabor, S. Sanders, S. Damm, D. W. Lantz, T. M. Lee, Z. Li, J.-M. Pratt, B. E. Price, and L. Seyda. 2008. *Movement and Habitat Use of Chinook Salmon Smolts, Northern Pikeminnow, and Smallmouth Bass near the SR 520 Bridge*. Lacey, WA: USFWS.

Chamberlin, J. W., T. E. Essington, J. W. Ferguson, and T. P. Quinn. 2011. "The Influence of Hatchery Rearing Practices on Salmon Migratory Behavior: Is the Tendency of Chinook Salmon to Remain within Puget Sound Affected by Size and Date of Release?" *Transactions of the American Fisheries Society* 140: 1398–408.

Chapman, M. G. 2003. "Paucity of Mobile Species on Constructed Seawalls: Effects of Urbanization on Biodiversity." *Marine Ecology Progress Series* 264: 21–9.

Chasco, B., I. C. Kaplan, A. Thomas, A. Acevedo-Gutierrez, D. Noren, M. J. Ford, M. B. Hansen, et al. 2017. "Estimates of Chinook Salmon Consumption in Washington State Inland Waters by Four Marine Mammal Predators from 1970 to 2015." *Canadian Journal of Fisheries and Aquatic Sciences* 74: 1173–94.

Cormack, R. M. 1964. "Estimates of Survival from Sighting of Marked Animals." *Biometrika* 51: 429–38.

Crooks, K. R., C. L. Burdett, D. M. Theobald, S. R. B. King, M. Di Marco, C. Rondinini, and L. Boitani. 2017. "Quantification of Habitat Fragmentation Reveals Extinction Risk in Terrestrial Mammals." *Proceedings of the National Academy of Sciences* 29: 7635–40.

Drinkwater, K. F., and K. T. Frank. 1994. "Effects of River Regulation and Diversion on Marine Fish and Invertebrates." *Aquatic Conservation: Marine and Freshwater Ecosystems* 4: 135–51.

Duffy, E. J., D. A. Beauchamp, and R. M. Buckley. 2005. "Early Marine Life History of Juvenile Pacific Salmon in Two Regions of Puget Sound." *Estuarine, Coastal and Shelf Science* 64: 94–107.

Espinoza, M., T. J. Farrugia, D. M. Webber, F. Smith, and C. G. Lowe. 2011. "Testing a New Acoustic Telemetry Technique to Quantify Long-Term, Fine-Scale Movements of Aquatic Animals." *Fisheries Research* 108: 364–71.

Fletcher, D. 2012. "Estimating Overdispersion When Fitting a Generalized Linear Model to Sparse Data." *Biometrika* 99: 230–7.

Furey, N. B., Hinch, S. G., Bass, A. L., Middleton, C. T., Minke-Martin, V., and Lotto, A. G. 2016. "Predator swamping reduces predation risk during nocturnal migration of juvenile salmon in a high-mortality landscape." *Journal of Animal Ecology* 85: 948–959.

Gaspar, P., and M. Lalire. 2017. "A Model for Simulating the Active Dispersal of Juvenile Sea Turtles with a Case Study on Western Pacific Leatherback Turtles." *PLoS One* 12(7): e0181595.

Gibson, A. J. F., E. A. Halfyard, R. G. Bradford, M. J. W. Stokesbury, and A. M. Redden. 2015. "Effects of Predation on Telemetry-Based Survival Estimates: Insights from a Study on Endangered Atlantic Salmon Smolts." *Canadian Journal of Fisheries and Aquatic Sciences* 72: 728–41.

Gillanders, B. M., K. W. Able, J. A. Brown, D. B. Eggleston, and P. F. Sheridan. 2003. "Evidence of Connectivity between Juvenile and Adult Habitats for Mobile Marine Fauna: An Important Component of Nurseries." *Marine Ecology Progress Series* 247: 281–95.

Haddad, N. M., L. A. Brudvig, J. Clobert, K. F. Davies, A. Gonzalez, R. D. Holt, and T. E. Lovejoy. 2015. "Habitat Fragmentation and Its Lasting Impact on Earth's Ecosystems." *Science Advances* 1: e1500052.

Halfyard, E. A., A. J. F. Gibson, D. E. Ruzzante, M. J. W. Stokesbury, and F. G. Whoriskey. 2012. "Estuarine Survival and Migratory Behavior of Atlantic Salmon *Salmo salar* Smolts." *Journal of Fish Biology* 81: 1626–45.

Hall, C. J., A. Jordaan, and M. G. Frisk. 2011. "The Historic Influence of Dams on Diadromous Fish Habitat with a Focus on River Herring and Hydrologic Longitudinal Connectivity." *Landscape Ecology* 26: 95–107.

Healey, M. C., and C. Groot. 1987. "Marine Migration and Orientation of Ocean-Type Chinook and Sockeye Salmon." *American Fisheries Society Symposium* 1: 298–312.

Hostetter, N. J., A. F. Evans, D. D. Roby, and K. Collis. 2012. "Susceptibility of Juvenile Steelhead to Avian Predation: The Influence of Individual Fish Characteristics and River Conditions." *Transactions of the American Fisheries Society* 141: 1586–99.

Jefferson, S., M. Smultea, E. Ward, and B. Berejikian. 2021. "Estimating the Stock Size of Harbor Seals (*Phoca vitulina richardii*) in the Inland Waters of Washington State Using Line-Transect Methods." *PLoS One* 16(6): e0241254.

Jeffries, S., H. Huber, J. Calambokidis, and J. Laake. 2003. "Trends and Status of Harbor Seals in Washington State: 1978–1999." *Journal of Wildlife Management* 67: 207–18.

Jolly, G. M. 1965. "Explicit Estimates from Capture–Recapture Data with Both Death and Immigration: Stochastic Model." *Biometrika* 52: 225–47.

Kendall, N. W., G. W. Marston, and M. M. Klungle. 2017. "Declining Patterns of Pacific Northwest Steelhead Trout (*Oncorhynchus mykiss*) Adult Abundance and Smolt Survival in the Ocean." *Canadian Journal of Fisheries and Aquatic Sciences* 74: 1275–90.

Khangaonkar, T., A. Nugraha, and T. Wang. 2018. "Hydrodynamic Zone of Influence Due to a Floating Structure in a Fjordal Estuary—Hood Canal Bridge Impact Assessment." *Journal of Marine Science and Engineering* 6: 119. https://doi.org/10.3390/jmse604119

Klinard, N. V., and J. K. Matley. 2020. "Living until Proven Dead: Addressing Mortality in Acoustic Telemetry Research." *Reviews in Fish Biology and Fisheries* 30: 485–99.

Laake, J. L. 2013. *RMark: An R Interface for Analysis of Capture-Recapture Data with MARK*. AFSC Processed Rep 2013-01. Seattle, WA: Alaska Fisheries Science Center, NOAA, National Marine Fisheries Service.

Lacroix, G. L. P., P. McCurdy, and D. Knox. 2004. "Migration of Atlantic Salmon Postsmolts in Relation to Habitat Use in a Coastal System." *Transactions of the American Fisheries Society* 133: 1455–71.

Lance, M. M., W. Y. Chang, S. J. Jeffries, S. F. Pearson, and A. Acevedo-Gutiérrez. 2012. "Harbor Seal Diet in Northern Puget

Sound: Implications for the Recovery of Depressed Fish Stocks." *Marine Ecology Progress Series* 464: 257–71.

Leander, J., J. Klaminder, G. Hellström, and M. Jonsson. 2021. "Bubble Barriers to Guide Downstream Migrating Atlantic Salmon (*Salmo salar*): An Evaluation Using Acoustic Telemetry." *Ecological Engineering* 160: 106141.

Meckley, T. D., E. Gurarie, J. R. Miller, and C. M. Wagner. 2017. "How Fishes Find the Shore: Evidence for Orientation to Bathymetry from the Non-Homing Sea Lamprey." *Canadian Journal of Fisheries and Aquatic Sciences* 75: 2045–58.

Melnychuk, M. C. 2009. "Mortality of Migrating Pacific Salmon Smolts in Southern British Columbia, Canada." Dissertation, University of British Columbia.

Moore, M. E., and B. A. Berejikian. 2013. "A Floating Bridge Disrupts Seaward Migration and Increases Mortality of Steelhead Smolts in Hood Canal, Washington State." *PLoS One* 8(9): e73427.

Moore, M. E., and B. A. Berejikian. 2017. "Population, Habitat, and Marine Location Effects on Early Marine Survival and Behavior of Puget Sound Steelhead Smolts." *Ecosphere* 8(5): e01834.

Moore, M., and B. Berejikian. 2022. "Coastal Infrastructure Alters Behavior and Increases Predation Mortality of Threatened Puget Sound Steelhead Smolts." Dryad. Dataset. https://doi.org/10.5061/dryad.8pk0p2npn.

Moore, M. E., B. A. Berejikian, and E. P. Tezak. 2010. "Early Marine Survival and Behavior of Steelhead Smolts through Hood Canal and the Strait of Juan de Fuca." *Transactions of the American Fisheries Society* 139: 49–61.

Moore, M. E., B. A. Berejikian, F. A. Goetz, A. G. Berger, S. S. Hodgson, E. J. Connor, and T. P. Quinn. 2015. "Multi-Population Analysis of Puget Sound Steelhead Survival and Migration Behavior." *Marine Ecology Progress Series* 537: 217–32.

Moore, M. E., B. A. Berejikian, C. M. Greene, and S. Munsch. 2021. "Environmental Fluctuation and Shifting Predation Pressure Contribute to Substantial Variation in Early Marine Survival of Steelhead." *Marine Ecology Progress Series* 662: 139–56.

Munsch, S. H., J. R. Cordell, J. D. Toft, and E. E. Morgan. 2014. "Effects of Seawalls and Piers on Fish Assemblages and Juvenile Feeding Behavior." *North American Journal of Fisheries Management* 34: 814–27.

National Marine Fisheries Service. 2019. *ESA Recovery Plan for the Puget Sound Steelhead Distinct Population Segment (Oncorhynchus mykiss)*. Seattle, WA: National Marine Fisheries Service.

Nehlsen, W., J. E. Williams, and J. A. Lichatowich. 1991. "Pacific Salmon at the Crossroads: Stocks at Risk from California, Oregon, Idaho, and Washington." *Fisheries* 162: 4–21.

Nelson, B. W., C. J. Walters, A. W. Trites, and M. K. McAllister. 2019. "Wild Chinook Salmon Productivity Is Negatively Related to Seal Density and Not Related to Hatchery Releases in the Pacific Northwest." *Canadian Journal of Fisheries and Aquatic Sciences* 76: 447–62.

Nilsson, C., C. A. Reidy, M. Dynesius, and C. Revenga. 2005. "Fragmentation and Flow Regulation of the world's Large River Systems." *Science* 308: 405–8.

Olds, A. D., R. M. Connolly, K. A. Pitt, S. J. Pittman, P. S. Maxwell, C. M. Huijbers, B. R. Moore, et al. 2016. "Quantifying the Conservation Value of Seascape Connectivity: A Global Synthesis." *Global Ecology and Biogeography* 25: 3–15.

Perry, R. W., J. R. Skalski, P. L. Brandes, P. T. Sandstrom, A. P. Klimley, A. Ammann, and B. MacFarlane. 2010. "Estimating Survival and Migration Route Probabilities of Juvenile Chinook Salmon in the Sacramento-San Joaquin River Delta." *North American Journal of Fisheries Management* 30: 142–56.

Peterson, J. H., and D. L. DeAngelis. 2000. "Dynamics of Prey Moving through a Predator Field: A Model of Migrating Juvenile Salmon." *Mathematical Biosciences* 165: 97–114.

Polis, G. A., W. B. Anderson, and R. D. Holt. 1997. "Toward an Integration of Landscape and Food Web Ecology: The Dynamics of Spatially Subsidized Food Webs." *Annual Review of Ecological Systems* 28: 289–316.

Port Gamble S'Klallam Tribe. 2021. *Appendix X: Factors Impacting Juvenile Salmon Migration at the Hood Canal Bridge*. Hood Canal Bridge Ecosystem Assessment Phase I Report. Seattle WA: Long Live the Kings.

Quinn, T. P. 2005. *The Behavior and Ecology of Pacific Salmon and Trout*. Seattle, Washington: University of Washington Press.

R Core Team. 2019. *R: A Language and Environment for Statistical Computing*. Vienna: R Foundation for Statistical Computing. https://www.R-project.org/

Romine, J. G., R. W. Perry, S. V. Johnston, C. W. Fitzer, S. W. Pagliughi, and A. R. Blake. 2014. "Identifying when Tagged Fishes Have Been Consumed by Piscivorous Predators: Application of Multivariate Mixture Models to Movement of Telemetered Fishes." *Animal Biotelemetry* 2: 3.

Roy, R., J. Beguin, C. Argiller, L. Tissot, F. Smith, S. Smedbol, and E. De-Oliveira. 2014. "Testing the VEMCO Positioning System: Spatial Distribution of the Probability of Location and the Positioning Error in a Reservoir." *Animal Biotelemetry* 2: 1–6.

Ruff, C. P., J. H. Anderson, I. M. Kemp, N. W. Kendall, P. A. McHugh, A. Velez-Espino, C. M. Greene, et al. 2017. "Salish Sea Chinook Salmon Exhibit Weaker Coherence in Early Marine Survival Trends than Coastal Populations." *Fisheries Oceanography* 26: 625–37.

Sabal, M. C., M. S. Boyce, C. L. Charpenter, N. B. Furey, T. M. Luhring, H. W. Martin, M. C. Melnychuk, et al. 2021. "Predation Landscapes Influence Migratory Prey Ecology and Evolution." *Trends in Ecology & Evolution* 36: 737–49.

Seber, G. A. F. 1965. "A Note on the Multiple-Recapture Census." *Biometrika* 52: 249–59.

Sheaves, M. 2009. "Consequences of Ecological Connectivity: The Coastal Ecosystem Mosaic." *Marine Ecology Progress Series* 391: 107–15.

Shepard, D. B., A. R. Kuhns, M. J. Dreslik, and C. A. Philips. 2008. "Roads as Barriers to Animal Movement in Fragmented Landscapes." *Animal Conservation* 11: 288–96.

Simenstad, C. A., K. L. Fresh, and E. O. Salo. 1982. "The Role of Puget Sound and Washington Coastal Estuaries in the Life History of Pacific Salmon: An Unappreciated Function." In *Estuarine Comparisons*, edited by V. S. Kennedy, 343–64. New York: Academic Press.

Skalski, J. R., J. Lady, R. Townsend, A. E. Giorgi, J. R. Stevenson, C. M. Peven, and R. D. McDonald. 2001. "Estimating in-River Survival of Migrating Salmonid Smolts Using Radiotelemetry." *Canadian Journal of Fisheries and Aquatic Sciences* 55: 1484–93.

Smith, F. 2013. *Understanding HPE in the Vemco Positioning System (VPS)*. Vemco Document No. DOC-005457-01. Bedford, Nova Scotia: Vemco Ltd.

Sobocinski, K. L., J. R. Cordell, and C. A. Simenstad. 2010. "Effects of Shoreline Modification on Supratidal Macroinvertebrate Fauna on Puget Sound, Washington, Beaches." *Estuaries and Coasts* 33: 699–711.

Sobocinski, K. L., N. W. Kendall, C. M. Greene, and M. W. Schmidt. 2020. "Ecosystem Indicators of Marine Survival in Puget Sound Steelhead Trout." *Progress in Oceanography* 188: 102419.

Sogard, S. M. 1997. "Size-Selective Mortality in the Juvenile Stage of Teleost Fishes: A Review." *Bulletin of Marine Science* 60: 1129–57.

Steel, A. E., P. T. Sandstrom, P. L. Brandes, and A. P. Klimley. 2013. "Migration Route Selection of Juvenile Chinook Salmon at the Delta Cross Channel, and the Role of Water Velocity and Individual Movement Patterns." *Environmental Biology of Fishes* 96: 215–24.

Stocking, J. J., and S. F. Pearson. 2019. "Appendix C: Evaluating the Potential Influence of the Hood Canal Bridge on Piscivorous Bird and Mammal Density." In *Hood Canal Bridge Ecosystem Assessment Phase 1 Report*. Seattle, WA: Long Live the Kings.

Thomas, A. C., B. W. Nelson, M. M. Lance, B. E. Deagle, and A. W. Trites. 2016. "Harbour Seals Target Juvenile Salmon of Conservation Concern." *Canadian Journal of Fisheries and Aquatic Sciences* 74: 907–21.

Thorstad, E. B., I. Uglem, P. Arechavala-Lopez, F. Økland, and B. Finstad. 2011. "Low Survival of Hatchery-Released Atlantic Salmon Smolts during Initial River and Fjord Migration." *Boreal Environment Research* 16: 115–20.

Thorstad, E. B., F. Whoriskey, I. Uglem, A. Moore, A. H. Rikarsen, and B. Finstad. 2012. "A Critical Life Stage of the Atlantic Salmon *Salmo salar*: Behavior and Survival during the Smolt and Initial Post-Smolt Migration." *Journal of Fish Biology* 81: 500–42.

Toft, J. D., J. R. Cordell, C. A. Simenstad, and L. A. Stamatiou. 2007. "Fish Distribution, Abundance, and Behavior Aslong City Shoreline Types in Puget Sound." *North American Journal of Fisheries Management* 27: 465–80.

Trombulak, S. C., and C. A. Frissell. 2000. "Review of Ecological Effects of Roads on Terrestrial and Aquatic Communities." *Conservation Biology* 14: 18–30.

Vargas-Fonseca, E., A. D. Olds, B. L. Gilby, R. M. Connolly, D. S. Schoeman, C. M. Huijbers, G. A. Hyndes, and T. A. Schlacher. 2016. "Combined Effects of Urbanization and Connectivity on Iconic Coastal Fishes." *Biodiversity Research* 22: 1328–41.

Ward, B. R. 2000. "Declivity in steelhead (Oncorhynchus mykiss) recruitment at the Keogh River over the past decade." *Canadian Journal of Fisheries and Aquatic Sciences* 57(2): 298–306.

Wargo Rub, A. M., N. A. Som, M. J. Henderson, B. P. Sandford, D. M. Van Doornik, D. J. Teel, M. J. Tennis, O. P. Langness, B. K. van der Leeuw, and D. D. Huff. 2019. "Changes in Adult Chinook Salmon (*Oncorhynchus tshawytscha*) Survival within the Lower Columbia River amid Increasing Pinniped Abundance." *Canadian Journal of Fisheries and Aquatic Sciences* 76: 1862–73.

Welch, D. W., M. C. Melnychuk, E. R. Rechisky, A. D. Porter, M. C. Jacobs, A. Ladouceur, R. S. McKinley, and G. D. Jackson. 2009. "Freshwater and Marine Migration and Survival of Endangered Cultus Lake Sockeye Salmon (*Oncorhynchus nerka*) Smolts Using POST, a Large-Scale Acoustic Telemetry Array." *Canadian Journal of Fisheries and Aquatic Sciences* 66: 736–50.

Wells, B. K., J. A. Santorra, M. J. Henderson, P. Warzybok, J. Jahncke, R. W. Bradley, D. D. Huff, et al. 2017. "Environmental Conditions and Prey Switching by a Seabird Predator Impact Juvenile Salmon Survival." *Journal of Marine Systems* 174: 53–64.

White, G. C., and K. P. Burnham. 1999. "Program MARK: Survival Estimation from Populations of Marked Animals." *Bird Study* 46(Suppl): 120–38.

Wieskotten, S., B. Mauck, L. Miersch, G. Denhardt, and W. Hanke. 2011. "Hydrodynamic Discrimination of Wakes Caused by Objects of Different Size or Shape in a Harbor Seal (*Phoca vitulina*)." *Journal of Experimental Biology* 214: 1922–30.

Wilcove, D. S., and M. Wikelski. 2008. "Going, going, gone: Is animal migration disappearing." *PLoS Biology* 6(7): e188.

Yurk, H., and A. W. Trites. 2000. "Experimental Attempts to Reduce Predation by Harbor Seals on out-Migrating Juvenile Salmon." *Transactions of the American Fisheries Society* 129: 1360–6.

Zimmerman, M. S., J. R. Irvine, M. O'Neill, J. H. Anderson, C. M. Greene, J. Weinheimer, M. Trudel, and K. Rawson. 2015. "Spatial and Temporal Patterns in Smolt Survival of Wild and Hatchery Coho Salmon in the Salish Sea." *Marine and Coastal Fisheries: Dynamics, Management, and Ecosystem Science* 7: 116–34.

SUPPORTING INFORMATION

Additional supporting information may be found in the online version of the article at the publisher's website.

How to cite this article: Moore, Megan E., and Barry A. Berejikian. 2022. "Coastal Infrastructure Alters Behavior and Increases Predation Mortality of Threatened Puget Sound Steelhead Smolts." *Ecosphere* 13(4): e4022. https://doi.org/10.1002/ecs2.4022